Aus dem Lehrstuhl für Tissue Engineering & Regenerative Medizin

der Universität Würzburg

Direktor: Prof. Dr. human. biol. Heike Walles

Development of a Dialysis Graft Based on Tissue Engineering Methods

Inaugural - Dissertation

zur Erlangung der Doktorwürde der

Medizinischen Fakultät

der

Julius-Maximilians-Universität Würzburg

vorgelegt von

Dejan Radaković

aus Bihać

Würzburg, 2018

Referentin: Prof. Dr. Heike Walles

Korreferentin: Prof. Dr. Jürgen Groll

Dekan: Prof. Dr. Matthias Frosch

Tag der mündlichen Prüfung: 03.07.2020

Der Promovend ist Arzt.

To my late father who inspired me to be determined person,

to my doting mother without whom I would never be able to achieve my objectives and succeed in life.

Part of this work is used as part of publication in:

***Radakovic D**, Reboredo J, Helm M, Weigel T, Schurlein S, Kupczyk E, et al. A multilayered electrospun graft as vascular access for hemodialysis. PLoS One. 2017;12(10):e0185916.*

Figures in this work which are also used for publication are suitably marked.

Part of this work is presented on conference:

IZKF-Retreat 19.-20. Mai 2017. Kloster Banz

Oral presentation: Development of a Dialysis Graft based on tissue engineering methods.

***Radakovic** D, Weigel T, Schurlein S, Walles H, Hansmann J*

Table of Contents

List of abbreviations

°C	Celsius
acLDL	acetylated-low density lipoprotein
AV	arteriovenous
CD31	Cluster of Differentiation 31
CKD	Chronic kidney disease
CO_2	Carbon dioxide
DAPI	4',6-diamidino-2-phenylindole
DMSO	Dimethyl sulfoxide
DNA	deoxyribonucleic acid
ECM	extracellular matrix
ECs	endothelial cells
EDTA	Ethylenediaminetetraacetic acid
EPS	extracellular polymeric substance
ePTFE	expanded polytetrafluoroethylene
EtOH	Ethanol
FCS	Fetal calf serum
FDA	Food and Drug Administration
HCl	Hydrochloric acid
HD	hemodialysis
HE	Hematoxylin and eosin staining
HFIP	1,1,1,3,3,3-Hexafluoro-2-propanol
HMDI	Hexamethylene diisocyanate
hmvECs	human microvascular endothelial cells

MACS	Magnetic Activated Cell Sorting
MTT	(3-(4,5-dimethyl-2-thiazolyl)-2,5-diphenyl-2H-tetrazolium bromide
PBS^-	phosphate buffered saline without calcium chloride and magnesium chloride
PBS^+	phosphate buffered saline with calcium chloride and magnesium chloride
PCL	Polycaprolactone
pen/strep	Antibiotics penicillin and streptomycin
PET	polyethylene terephthalate
PFA	Paraformaldehyde
PGA	Polyglycolide
PI	Propiumbromiodide
PLGA	poly (lactic-co-glycolic acid)
PLLA	poly-L-lactide
rH	Relative humidity
rpm	Rounds per minute
RRT	renal replacement therapy
SEM	Scanning electron microscope
SMCs	smooth muscle cells
TE	tissue engineering
TEBV	tissue engineered blood vessels
TEVG	tissue-engineered vascular graft
TFE	trifluoroethanol
VE water	Fully demineralized water
vWF	von-Willebrand-Faktor

1. Introduction

Evolution of diagnostic tests, drugs, interventional catheter-based techniques as well as ventricular assist devices has advanced cardiovascular medicine to such an extent that few people anticipated in 1950s and 1960s when this medical field still was in its infancy. On the other side, bypass surgery remained almost unchanged. Modern techniques for peripheral and coronary artery bypass differ little from first procedures of this kind in middle of 20th century. Development of cardiovascular biomaterials has been similarly slow over the past few decades. The most spread is the use of biological autologous grafts, and when one is not available synthetic grafts are used. In 1950s Dr. DeBakey pioneered polyethylene terephthalate (PET) for repairing blood vessels (Figure 1), which was then used around the world. In a modern era of cardio-vascular surgery new options for vascular grafting are searched for. The most important milestones in development of vascular grafts as an access for hemodialysis are shown in Table 1. In the middle of 1980s

Figure 1. Dr. Michael E. DeBakey *at home sewing a Dacron artificial graft, 1955. (Image courtesy of Baylor College of Medicine Archives)*

Table 1. Milestones in development of vascular grafts and access for hemodialysis

First half of the 18th century	chemical styptic, cauterization, ligation
1759	first lateral arteriorrhaphy
1879	Eck performed a lateral anastomosis of the portal vein to the inferior vena cava
1896	Jaboulay and Briau sutured an artery end-to-end in dog
1912	Carrel was awarded the Nobel Prize for his work on vascular three-point end-to-end and a side-to-side-anastomosis, still used today
1924	Georg Haas (Giessen, Germany) performed the first hemodialysis treatment in humans which lasted 15 min
1942	Blakemore and Lord use vitalium tubes for non-suture anastomosis
1943	modern hemodialysis therapy started with the work of Willem Kolff Kunlin bypasses obstructed arteries with autogenous vein segments
1950s	the polyethylene terephthalate (PET) prosthesis (trademarked as Dacron® by DuPont) was pioneered by Michael E. DeBakey (Figure 1.)
1952	in Columbia-Presbyterian Hospital Vinyon—N tube used to replace ruptured artery
1960	Scribner developed an arteriovenous (AV) Teflon shunt
1961	Stanley Shaldon introduced hand-made catheters into the femoral artery and vein by the percutaneous Seldinger technique for immediate vascular access
1962	James E. Cimino and Michael J. Brescia described a ‘simple venipuncture for hemodialysis’
1963	Thomas J. Fogarty from Cincinnati, USA, invented an intravascular catheter with an inflatable balloon for embolectomy and thrombectomy
1968	Lars Röhl from Heidelberg, Germany, published his results in 30 radial-artery-side-to-vein-end-anastomoses
1969	development of expanded PTFE (ePTFE), trademarked as Gore-Tex® by Bob Gore
1976	L.D. Baker Jr. presented the first results with expanded PTFE grafts in 72 hemodialysis patients (2)

Bell and his colleagues postulated that cell-seeded living grafts could be grown in vitro, which was the first radical advancement for prosthetic graft design. (3) More than a

decade later, another group led by Shin'oka first applied this theory clinically and were able to successfully use cell-seeded polymers to repair congenital defects in the low-pressure pulmonary outflow tract of pediatric patients. (4, 5) Neither of these grafts showed sufficient mechanical strength so far to warrant application for the bypass (neither aorto-coronary nor peripheral) in adult surgery.

1.1. Problem of access for hemodialysis

Chronic kidney disease (CKD) has a high prevalence and incidence worldwide and in many patients, it leads to renal replacement therapy (RRT). The reasons for CKD are:

- Glomerulonephritis 40%
- Pyelonephritis 20%
- Kidney Cysts 8%
- Vascular pathology 5% (6)

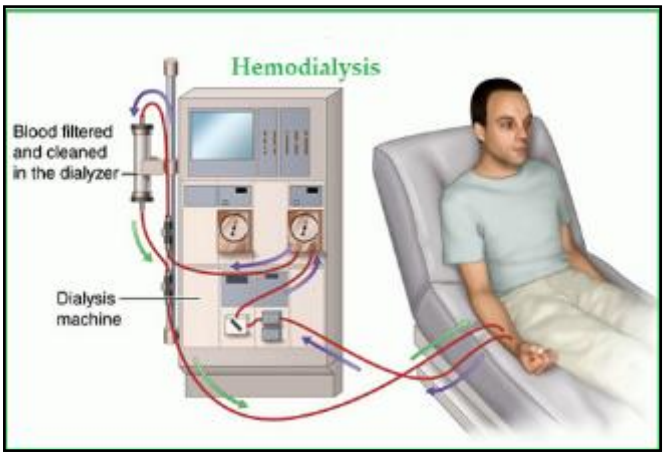

Figure 2. Typical setting for hemodialysis *(courtesy of Ehealthhut© www.ehealthhut.com).*

RRT is indicated when kidney function declines to the point that retention of waste substances leads to clinical signs and symptoms. The glomerular filtration rate (GFR) as indication for dialysis varies from center to center but is typically ≤ 10 ml/min/1.73m^2. RRT can be implemented through hemodialysis (HD) as shown in Figure 2, peritoneal dialysis (PD) and renal transplantation. Peritoneal dialysis allows patient home treatment and it uses the patient's peritoneum in the abdomen as a membrane across which fluids and dissolved substances are exchanged from blood. Hemodialysis achieves

extracorporeal removal of the waste. In addition to a growing number of patients with end-stage kidney disease, the number of surgical and interventional procedures required to establish and maintain arteriovenous vascular access to HD keeps rising. It is assessed that the number of patients on HD is growing 4 – 8% yearly worldwide, and diabetes mellitus (DM) is labeled as one of the leading causes.

At the initiation of hemodialysis, central venous catheters are the dominant form of vascular access. (7) Current clinical guidelines suggest an autogenous arteriovenous (AV) fistula as preferred vascular access in these patients. Thus, AV fistula represents one of the most common vascular surgery procedures performed worldwide. (8) AV fistula itself is abnormal connection between an artery and a vein. Such fistula can be:

- Congenital – defect in development (Sturge-Weber Syndrome)
- Result of penetrating injury
- Rupture of arterial aneurysm in an adjacent vein
- Surgically created for hemodialysis (for example Cimino fistula)

Surgically, AV fistula for hemodialysis can be created in different positions using different autologous vessels. The first fistula should be created as distal as possible in the forearm. The fistula is product of vascular anastomosis usually between a. radialis and v. cephalica in forearm, and a. brachialis and v. cephalica or a. brachialis and v. basilica in upper arm. The aim of such fistula is to provide the blood flow of 250 – 300 mL/min during the hemodialysis. Both the artery and vein dilate and elongate in response to shear stress, whereas veins more and become arterialized. This process is called maturation and it can last up to six weeks and during this period dialysis is usually performed using central venous catheter. After a month, it is expected that fistula can stand up to 700 – 1000 mL/min blood flow. Cimino fistula is made in forearm and the first requirement is good palpable pulse in a. radialis. The surgical procedure is performed with one S-form skin cut, after that v. cephalica is exposed (min. 5 cm in length), and then beneath the fascia a. radialis. The anastomosis made is most commonly end-to-side.

Most common complications of AV fistulas are:

- Thrombosis (17-25%)
- Aneurysms (5-6%)
- Steal syndrome (2-8%)
- Infection (2-3%)
- Cardiac failure (12-17%)
- Venous hypertension (9)

Unfortunately, many patients still lack a suitable vein grafts in arms for this procedure and they rely on chronic venous catheters or prosthetic AV grafts which carry a lifetime risk of thrombosis and infection, and as such are neither recommended nor discouraged in modern guidelines. Synthetic vascular grafts made from expanded polytetrafluoroethylene (ePTFE, Gore-Tex) or polyethylene terephthalate (PET, Dacron®) are very successive to replace large diameter blood vessels (≥ 6 mm), but they fail when used for replacement of small diameter blood vessels. (10-13) All causes for vascular graft failure can be classified into early, midterm and late. (14)

Early failures (31 – 61 %) are those that occur within 30 days of implantation:

- Technical complications
- Flow disturbances
- Acute thrombosis (15)

Midterm failure such as lumen occlusion due to intimal hyperplasia occurs from 3 months to 2 years after the graft implantation. Late failures occur after 2 years from implantation and are related to atherosclerotic disease.

The prosthetic grafts show mismatch in compliance compared to natural vessels, they lack antithrombogenic endothelial layer, and as a prosthetic material have predisposition to infection for the life of the graft. Therefore, infection, intimal hyperplasia and thrombosis often lead to graft failure and contribute to the high costs of renal replacement therapy. Intimal hyperplasia and thrombosis have been associated with inadequate endothelial cell coverage of the luminal surface of the vascular graft. (16) Thereafter,

autologous or allogenic transplantation is widely spread and preferred, but not always available and appropriate. For this reason, TE is trying to offer novel options for vascular grafting as shelf-ready alternative. (3)

Together with the increase of surgical interventions to establish a suitable hemodialysis access the number of surgical site infections, especially prosthetic graft infections are raising simultaneously so that nosocomial infection is one of the most serious complications in these patients and the second cause of death in dialysis patients. Despite the use of prophylactic antibiotics during modern surgeries, the incidence of graft infection remains up to 5 % after vascular graft implantation. (17) The mechanism for graft infection can be divided into three categories:

- perioperative contamination,
- postoperative wound infection or
- systemic bacteremia.

After graft infection, treatment traditionally consist of two stages: removal of infected graft and placement of dialysis catheter until the new access spot is created and maturated and initiation of systemic antibiotic therapy. One of important aspects of vascular graft infection is formation of biofilm on the vascular prosthesis. Biofilm is per definition any group of microorganisms in which cells interact to each other incorporated in extracellular polymeric substance (EPS), which acts as a barrier against antibiotics and hosts immune system, and such group of cells tend to adhere to surface. EPS is composed of polysaccharides and proteins, but also include other molecules, such as DNA and lipids. (18) Biofilms are formed as a response to many different factors. When a certain bacteria switches to biofilm growth, it makes a phenotypic shift and many genes are differentially regulated. This way, the same bacteria inside the biofilm express a distinct metabolic pathway and compared to metabolically active bacteria alone display a decreased antibiotics sensitivity. (19, 20) It is known that in case of *Staphylococcus aureus* infection for example, the sub-therapeutic levels of antibiotic, especially β-lactam antibiotics, induce the biofilm formation. (21) All this previously stated sums important reasons why antibiotics therapy only, without graft removal when biofilm is already formed is not sufficient in case of vascular graft infection and that explains the reason of recurrent

infections. With that in mind, development of infection resistant graft, at least to some extent, may further reduce the incidence of this complication by patients on hemodialysis.

1.2. Blood vessels anatomy

Tissue is a cellular organizational level intermediate between cells and a complete organ. It consists of cells embedded in an extracellular matrix (ECM), which is composed of proteins, glycoproteins, glycosaminoglycans and proteoglycans. The most abundant proteins in most tissue types are forms of collagen and elastin, with lesser amount of fibronectin, laminin, vitronectin and other ECM proteins. The interplay between specific cells and the ECM structure induces the formation of different tissue types with specific functions. Vascular TE aims to develop biological substitutes that can restore, maintain and improve tissue function in a manner identical to natural vessels. Therefore, it is important to understand the histological structure of human vasculature. Blood vessels are the part of the circulatory system that transports blood throughout human body. They have concentric layered structure, where every layer has typical organization of different cells and proteins:

- Tunica intima
- Tunica media
- Tunica adventitia

The luminal layer consists of specialized endothelial cells (ECs). This layer is called intima. Endothelial cells play also a key role in preventing the formation of clots and vascular thrombosis, as endothelial injury is an important part of Virchow's triad. It also plays an important role in preventing infection, inflammation and in signaling to the muscular component of the vessel wall through nitric oxide secretion. Nitric oxide is a signaling molecule which increases the activity of the second messenger cyclic guanosine monophosphate (cGMP) in smooth muscle cells, which then causes cell muscle relaxation and blood vessel dilatation.

The tunica media is separated from the intimal layer by a basal membrane, which consists mostly of laminin and collagen IV. In this layer, smooth muscle cells are concentrically

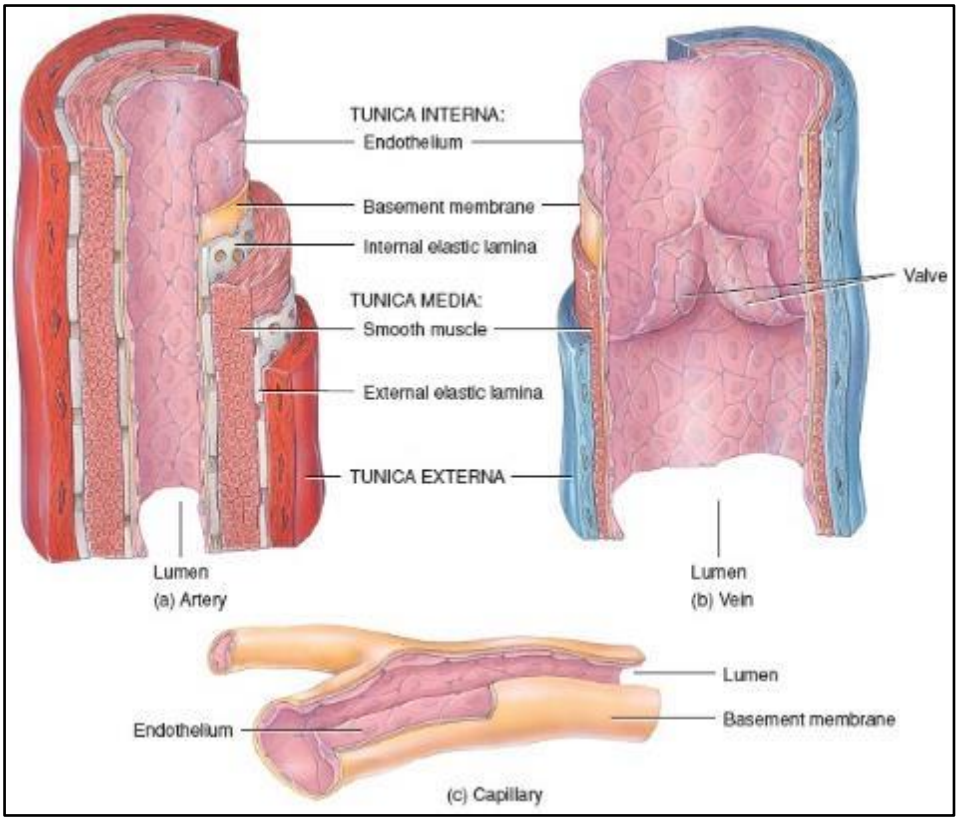

Figure 3. Blood vessels classification and structure. Copyright © 2011 John Wiley & Sons, Inc.

arranged, which have an important role in altering the vessel diameter and varying amounts of collagen fibers, elastic fibers and proteoglycans (amount and proportion of these depends of blood vessel type). The outer layer named tunica adventitia is mostly made of collagen fibers.

Collagens are divided into two categories: fibrillary types I, II, III and V as well as nonfibrillar collagens such as type IV. Collagen is three-chain fibrous protein in which the chains coil around each other like the strands of the rope. This triple-helix molecular organization generates a protein with considerable tensile strength. The defect of synthesis, processing and assembly of collagen is clinically significant and leads to hyperelasticity of the skin and hypermobility of the joints and is known as Ehlers-Danlos syndrome. (22)

All blood vessels (Figure 3) are classified as either:

- Arteries – thick, strong and contain muscles elastic fibers and fibrous tissue
- Capillaries – very thin, one cell layer
- Veins – thin, mainly fibrous tissue less muscle and elastic tissue

1.3. Tissue engineering and regenerative medicine

Regenerative medicine is working on clarification of different mechanisms, which define the function of various tissues and on the development of alternative strategies for the treatment of organ failure or organ loss. Due to the world-spread shortage of donor organs in transplantation medicine and the longer life expectancy, regenerative medicine is becoming increasingly important. Regenerative medicine has its origin in observations that certain species or also certain human tissues have regenerative capabilities. Tissue engineering is very young field of regenerative medicine aiming to create artificial tissues or organs to replace or restore the damaged organ combining scaffolds, cells and growth factors. For TE the best cell source should be non-immunogenic, functional and easy to achieve and expand in cell culture. For TE of vascular grafts the first choice is autologous endothelial cells (ECs) isolated from patients themselves. Although we are nowadays not only able to isolate most of the human cells, but also to differentiate them from multipotent stem cells, the initial idea came first in 1858 to Virchow, (23) who stated "Omnis cellula e cellula..", which meant that cells develop from the preexisting cells. The first idea of growing the cells outside the human body came with Loeb in 1897. (24) First success was survival of the cells in different media, with no growth, but later this was succeeded too, trends changed into further expanding the cells in vitro throughout 1940, which finally led to ability to grow tissue-specific cell lines in vitro. The development of stem cell lines by the end of 20th century formed the basis for the modern TE and regenerative medicine. (25)

The main concept of tissue engineering is shown in Figure 4. Primary cells are isolated from tissue biopsies usually from human donors, after that the cell number is expanded using different methods for cell cultivation. Finally, these cells are then seeded on scaffolds, and cultivated in bioreactors until maturation. The formed tissue or organ can be used for transplantation in human patient or as a biological test system. TE concept based on scaffolds often means combining viable cells, biomolecules and a structural scaffold, all combined to support repair or regeneration. The scaffolds are required to resemble the natural properties on which the cells can proliferate, organize and differentiate into appropriate cell types. The scaffold should be preferably absorbed from the surrounding tissue while simultaneously the new tissue is formed. This way, the scaffold is replaced by new tissue, overtaking its structure and mechanical load. (26) Bell and his colleagues postulated in the middle 80s that cell-seeded living vascular grafts could be grown in vitro. They also achieved sufficient endothelial lining and beside possibility of further in vitro studies of endothelial cells the usage of such vascular prothesis for small caliber arteries was postulated. (3)

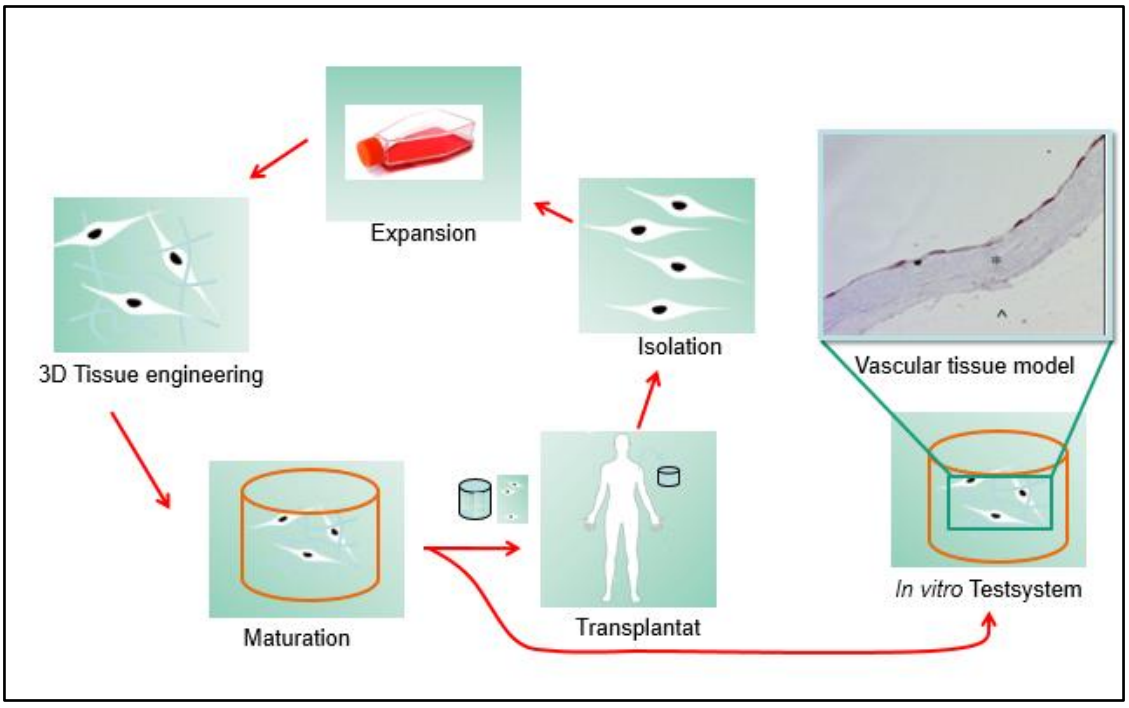

Figure 4. Main concept of TE. *Cells are isolated from a tissue biopsy of a patient. After expansion, cells are seeded on scaffolds for 3D tissue generation and then incubated and maturated in a bioreactor system. Generated artificial tissues can be used as 3D test system or transplanted back into patient. (modified from Seliger2015).*

Biomaterials used for making TE scaffolds can be classified into natural and synthetic biomaterials. Natural biomaterials are taken from their natural sources, whereas synthetic are developed and can be categorized into inorganic and organic. For the development of scaffolds, usually both kinds of biomaterials are used. Biomaterials need a good biocompatibility and must provide biological signals to cells so that cells attach and proliferate with a physiological viability. (27, 28) These are also good degradable, which represents advantage when tissue replacement is wished. Choosing the right solvent for biomolecules represents its disadvantage, as some of them tend to denaturate during electrospinnig as in case of collagen. (29) or they need specific treatments to be dissolved at all as silk for example. (30) Synthetic polymers are usually used to increase the mechanical stability and shape stability of the scaffolds. Such polymers are widely spread and many different have already been used. Choosing an appropriate solvent is also an easier task when working with synthetic polymers. Electrospun tubes of polyureathane are widely researched and used for vascular TE because of their suitable elastic nature and mechanical strength. Cell viability studies show also good biocompatibility of these scaffolds, whereas modifications with natural materials such as collagen showed superior results regarding cell viability on such scaffolds. (31)

The process of cells growing on scaffolds can be performed in a bioreactor system where in-vivo-like conditions are simulated and beside cell medium also a tissue-specific physiological in vitro environment is provided. This can be achieved with different bioreactor systems, where temperature is controlled at 37 °C, as in human body, gas atmosphere is stable and construct itself provides the transport of cell medium to all cells being cultivated no matter how big the tissue sample can be. Also the simulation of physiological conditions such as breathing, circulation or simply mechanical pressure may be required and as such provided in bioreactor for TE. (32) As a result, engineered tissues can be used as a 3D in vitro test system reducing the number of animal experiments, or used in vivo as an optimal graft to be implanted in patient and replace diseased, damaged or degenerated tissue.

There are different biological alternatives to vascular grafts, many were studied, but none of these has gained a wide acceptance. Some of the widely spread methodologies to create

a tissue-engineered blood vessels (TEBV) include endothelial cell lined scaffolds, polymer-based scaffolds and decellularized scaffolds. (33)

Bovine mesenteric vein grafts showed good results as temporary graft material in patients with graft site infections, but are unacceptable as definitive solution due to low short- and long-term patency rates and high risk of aneurysm formation. (34) Additionally, in one single center long-term study, decellularized bovine ureter grafts revealed that they are prone to stenosis and aneurysmal changes. (35) Bovine carotid arteries showed acceptable long-term patency rate but only in one-center studies with small study populations. For this reason, further investigations regarding this graft material are needed. (36) L'Heureux's group showed good patency rate and mechanical properties of completely autologous TEVG which were used as hemodialysis access in ten high-risk patients and so they showed that a tissue engineered blood vessel produced in vitro could withstand the challenges of arterial pressure produced by arteriovenous fistula for at least 3 months. (37) This was the important milestone for cardiovascular tissue engineering.

1.4. Electrospinning for tissue engineering

The concept of vascular TE is based on combining autologous vascular cells with a tubular scaffold under suitable culture conditions to mimic a native blood vessel. Such vascular scaffold having all or similar mechanical and biological properties as native vessel can be suitable alternative to autologous graft materials. One effective techniques to produce nanofibrous scaffolds is electrospinning, which allows fabrication of continuous nano- and microscale filaments. Electrospun scaffolds have certain additional characteristics which make them suitable for vascular TE, which are initial mechanical strength and stiffness, sufficient structural integrity during the tissue growth and remodeling process, microarchitecture suitable for initial cells attachment and subsequent migration into and through the matrix, good degradation and resorption kinetics needed for tissue development.

The process of electrospinning was first patented by J. F. Cooley in 1902. (38) After 1930s and some further adjusting, especially through the work of Anton Formhals, this technique received minor applicability until 1990s with growing interest in micro- and nanotechnology, when electrospinning experienced a "come back" to modern science. In

the early years of 1990s, several research groups demonstrated that many natural polymers can be electrospun into nanofibers with fiber size between 100 – 500 nm. (39) Only recently, the electrospinning has been also proposed and used for production of scaffolds in TE. (40, 41)

The process itself is based on appliance of high voltage to a liquid droplet, when the body of the liquid becomes charged, and electrostatic repulsion counteracts the surface tension and the droplet is stretched until at the critical point (formation of Taylor cone) a stream of liquid erupts from the surface and the jet is directed to a grounded collector. Typically, as shown on Figure 5, a high voltage is applied to a polymer solution that is pumped at the slow rate through the spinneret facing the collector. While going through the spinneret, due to voltage applied electrostatic repulsion counteracts the surface tension and the droplet is stretched, at this point the Taylor cone is formed on the tip of spinneret. Further on, a continuous jet is ejected and drown to the collector. Voltage, potential difference between the two spinnerets ranges between 10 and 20 kV, whereas even values between 0.5 to 130 kV have been reported. (42, 43) During the flight through the air jet

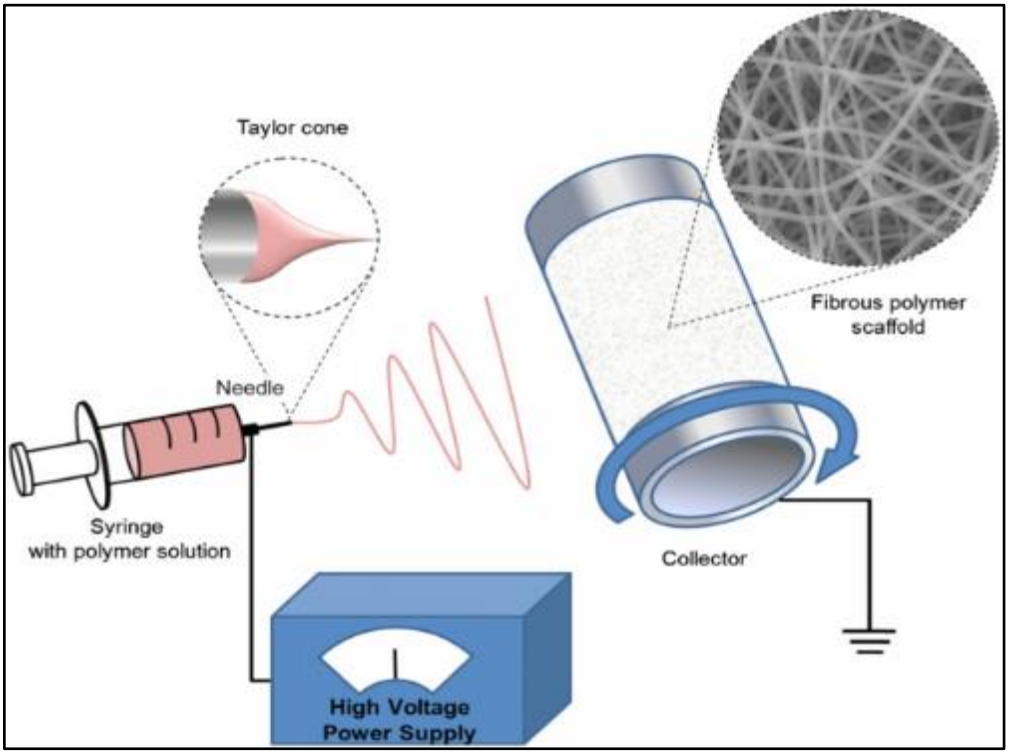

Figure 5. Schematic of typical electrospinning setup *(taken from Nae Gyune Rim et al Current approaches to electrospun nanofibers for tissue engineering 2013 Biomed. Mater. 8)*

is polymerized, elongated, and thinned resulting the formation of uniform nanofibers. Electrospinning can be performed so that the orientation of spinneret and collector is either horizontal or vertical. Although the fiber flight and collection is dynamic and rapid process and possibilities to manage it may seem technically challenging, one can produce either chaotic or organized fibers with defined orientation depending on the electrospinning setting is used. An alternative to solution electrospinning is melt electrospinning. During melt electrospinning, stable region of the jet is much longer and the larger diameter fibers are produced. (44)

Important parameters defining fiber size and morphology are polymer concentration in the solution, voltage applied on solution and environment conditions such as: humidity, temperature, absolute pressure. All these different factors have major influence on fiber morphology sequentially playing the important role on scaffold morphology. Solution viscosity plays the most important role in determining the fiber size and morphology during electrospinning. At low polymer concentrations the process itself is characterized more as electrospraying. (45) The diameter of the fibers was found to increase with the increase of solution concentration. (46) It is shown that poly-L-lactide (PLLA) fibers had 100 –300 nm diameter when produced from 1 wt.%, whereas diameter increased to 800 – 2400 nm by increasing the concentration to 5 wt.%. (47) Further on, it is known that low flow rate leads to fibers with smaller diameters, whereas higher rates produce fibers that dry first after reaching the collector and tend to have slightly higher rates. (48) In different studies it was demonstrated that at too high voltage or when the distance between spinneret tip and collector is too close or too high, formation of beads was observed. (49, 50) Also, ambient parameters are known to show effects on the electrospinning process. An increased temperature during electrospinning leads to production of smaller fibers due to decrease in solution viscosity, and increased humidity is known to cause circular pores formation on fibers. (51, 52)

Many different polymers have been studied for TEBV with the methods of electrospinning such as Polylactic acid (PLA), Polyglycolide (PGA), poly (lactic-co-glycolic acid) (PLGA) and Polycaprolactone (PCL). PCL was chosen in this experiment because it is a slowly degrading polymer (~2 – 3 years), has already Food and Drug Administration (FDA) approval in specific applications used in the human body as drug

delivery device or suture. It is also biocompatible and poses good mechanical properties needed for development of TEVG. Beside the PCL, the natural polymer collagen Type I was used, as the main structural protein in the extracellular space in vascular tissue.

2. Aim of the study

Despite advancements of modern medicine, the number of patients with the the end-stage kidney disease keeps growing, and surgical procedures to establish and maintain a vascular access for hemodialysis are rising accordingly. (53) Surgical access of choice remains autogenous arteriovenous fistula, whereas approach “fistula first at all costs” leads to failure in certain subgroups of patients. (54) Modern synthetic vascular grafts fail to deliver long-term results comparable with AV fistula. With all that in mind, this work has an aim of developing a new alternative vascular graft which can be used for hemodialysis access using the methods of TE, especially electrospinning technique. It is hypothesized that electrospun scaffold, made of PCL and collagen type I may assemble mechanical properties similar to native blood vessels. Seeding such electrospun scaffolds with human microvascular endothelial cells (hmvECs) and preconditioning with shear stress and continuous flow might achieve sufficient endothelial lining being able to resist acute thrombosis. Important aim at this step is finding the best suitable polymer concentration for production of scaffold with the best bioavailability properties. All that represents themes in which the whole work can be divided: scaffold production using different electrospinning settings, testing mechanical and biological properties of these scaffolds, 2D tests with hmvECs, and finally work with the most proper scaffold on a production of 3D tissue model using the dynamic bioreactor system with continuous flow. One further topic considered on-site infections which represents one of the most spread complications of dialysis therapy due to continuous needle punctures. The main hypothesis was that during electrospinning process, polymers can be blended with antibiotics with the aim of producing scaffolds with antimicrobial properties, which could lead to reducing the risk of on-site infection on one side, while not affecting the cell viability.

3. Materials

The biological materials, antibodies, enzymes, experimental kits, chemicals and solutions as well laboratory materials, equipment/devices and software used for this study are all listed in the following tables.

3.1. Biological materials

For all cell experiments, the human microvascular endothelial cells (hmvECs) were isolated from foreskin biopsies after circumcision. The procedure was approved by the ethical commission of the University of Wuerzburg (vote 182/10).

3.2. Chemicals and solutions

General chemicals, solutions and buffers, which were used are shown in Table 2.

Table 2. List of chemicals, solutions and buffers

Chemical/Solution	Manufacturer
Acetic acid, 100 %	Carl Roth, Karlsruhe (GER)
Acetic acid (glacial), 100 %	Merck, Darmstadt (GER)
Acetone, ≥ 99.5 %	Carl Roth, Karlsruhe (GER)
Albumin fraction V (BSA)	Carl Roth, Karlsruhe (GER)
Antibody diluent	Dako, Hamburg (GER)
DAPI fluoromount-GTM	SoutherinBiotech, Birmingham (USA)
Deionized water	Tissue Engineering and Regenerative Medicine, Würzburg(GER)
Dimethyl sulfoxide (DMSO)	Sigma-Aldrich, Seelze (GER)
Donkey serum	Sigma-Aldrich, Seelze (GER)
Dulbecco's phosphate buffered saline with calcium chloride and magnesium chloride (PBS^+)	Sigma-Aldrich, Seelze (GER)

Dulbecco's phosphate buffered saline without calcium chloride and magnesium chloride (PBS^-)	Sigma-Aldrich, Seelze (GER)
Entellan®	Merck, Darmstadt (GER)
Eosin Ethanol, absolute	Sigma-Aldrich, Seelze (GER) Carl Roth, Karlsruhe (GER)
Ethanol, denaturated, 96 %	Carl Roth, Karlsruhe (GER)
Ethylenediaminetetraacetic acid (EDTA)	Sigma-Aldrich, Seelze(GER)
Fetal calf serum (FCS)	Lonza, Köln (GER)
Fluoresceindiacetat (FDA)	Sigma Aldrich (GER)
Gentamicinsulfat, 40 mg	Merck Serono GmbH, Darmstadt (GER)
H_2O_2, 30 %	Carl Roth, Karlsruhe (GER)
Hematoxylin(Mayer)	Carl Roth, Karlsruhe (GER)
HMDI	Sigma-Aldrich, Seelze(GER)
Hydrochloric acid (HCl), 37 %, 1M	VWR, Darmstadt (GER)
LIVE/DEAD® Viability/Cytotoxicity Kit	Invitrogen, Darmstadt (GER)
Mowiol	Carl Roth, Karlsruhe (GER)
MTT (3-(4,5-dimethyl-2-thiazolyl)-2,5-diphenyl-2H-tetrazolium bromide)	Serva, Heidelberg (GER)
Paraformaldehyde (PFA)	AppliChem, Darmstadt (GER)
Penicillin (10,000 U/ml)/Streptomycin (10 mg/ml), 100x	PAA, Cölbe (GER)
2-Propanol	Carl Roth, Karlsruhe (GER)
Propiumbromiodide (PI)	Sigma Aldrich (GER)
Roti®-Histofix	Carl Roth, Karlsruhe (GER)
Sodium deoxycholate	Carl Roth, Karlsruhe (GER)
Tissue Tek® O.C.T. Compound	Weckert, Kitzingen (GER)
Triton-X 100	Carl-Roth, Karlsruhe (GER)
Trypan blue, 0.4 %	Sigma-Aldrich, Seelze (GER)
Tween-20	VWR, Darmstadt (GER)

Ultrapure water	Millipore, Schwalbach (GER)
Vancomycin CP 500mg	Hikma Pharma GmbH, Graefelfing (GER)
VascuLife® (VEGF endothelial cell culture medium)	CellSystems GmbH, Troisdorf (GER)
Versene solution	Gibco, Darmstadt (GER)

3.3. Media, solutions and buffers for cell culture

In Table 3, media, solutions and buffers used for cell culture are shown.

Table 3. List of media, solutions and buffers used for cell culture

Medium/Solution	Composition
VascuLife®	5 ng/ml rh VEGF LifeFactor 5 ng/ml rh FGF basic LifeFactor 15 ng/ml rh IGF-1 LifeFactor 5 ng/ml rh EGFLifeFactor 50 ng/ml Ascorbic acidLifeFactor 1 µg/ml Hydrocortisone 10 mM hemisuccinate LifeFactor 0.75 U/ml L-glutamineLifeFactor 2% (v/v) HeparinSulfate LifeFactor FCS in VascuLife®basal medium
Dispase solution	Dispase in PBS^- 2.00 U/ml
MTT reagent	MTT in cell culture medium 1 mg/ml
PBS^- pH 7.2	NaCl 140,00 mM KCl 2,00 mM KH2PO4 1,50 mM Na2HPO4 x 2 H2O 6,50 mM MgCl2 x 6 H2O 0,50 mM CaCl2 0.90 mM in ddH2O

PBS^-/EDTA solution	EDTA, 0.54 M in PBS^- 0.1 % (v/v)
Transport medium	PBS^+ with 1% Gentamycin
Trypsin/EDTA working solution	Trypsin-EDTA, 0.5 % in PBS^-/EDTA 0.05 % (v/v)

3.4. Solutions and buffers for histology and immunohistochemistry

All solutions and buffers, which were used for histological and immunohistological experiments, are showed in Table 4.

Table 4. Solutions and buffers used for histology and immunohistochemistry

Medium/Solution	Composition
Acetic acid, 3 %	3 % (v/v) Acetic acid, 100 % in deionized water
Eosin	10 mg/ml Eosin in deionized water
EtOH/Acetone	50 % (v/v) Ethanol, denaturated 50 % (v/v) Acetone, ≥ 99.5 %
H2O2, 3 %(v/v)	3 % (v/v) H2O2, 30 % in deionized water (prepared immediately before use)
HCl/EtOH (used for hematoxylin and eosin (H&E) staining)	6.85 % (v/v) HCl, 1M in 50 % (v/v) ethanol
Hemalaun(Mayer)	1.2 mg/ml Hematoxylin 0.2 mg/ml NaIO3 20 mg/ml Potassium alum 20 mg/ml Chloral hydrate 1 mg/ml Citric acid in deionized water

	(used after 4 weeks of maturation)
PBST, 0.05 M	0.5 % (v/v) Tween-20 in 1x PBS, pH 7.4
Tris buffered solution (TBS) Stock, 0.5 M (10x concentrated)	78.87 g/l Trizma hydrochloride 87.66 g/l NaCl in ultrapure water
Triton-X permeabilizing solution	0.02 % (v/v) Triton-X 100 in 0.05 M TBS buffer

3.5. Antibodies

Antibodies used for immunofluorescence (IF) are listed in Table 5.

Table 5. List of antibodies used for phenotypic characterization of hmvECs

Antigen	Host	Applied dilution	Manufacturer
CD31	Rabbit	1:500	Dako, Hamburg (GER)
Collagen I	Mouse	1:200	Acris, Herford (GER)
vWF	Rabbit	1:200	Abcam, Cambridge (GB)

3.6. Laboratory materials and equipment

Used laboratory materials and equipment in this study are listed in Table 6.

Table 6. Laboratory materials and equipment

Laboratory material	Manufacturer
Aspiration Device: VacuBoy	Integra Biosciences, Fernwald (GER)
CD31 MicroBead Kit	Miltenyi Biotec GmbH, (GER)
Cell Incubator: 37 °C, 5 % CO_2	Heraeus, Hanau (GER)
Centrifuges: Multifuge X3R Centrifuge 5417R Centrifuge 5424	 Thermo Fisher Scientific, Dreieich (GER) Eppendorf, Hamburg (GER) Eppendorf, Hamburg (GER)

Cell crowns	Chair of Tissue Engineering & Regenerative Medicine, University Hospital Würzburg (GER)
Cold-Storage Room, 4 °C	Genheimer, Hochberg (GER)
Contact angle measuring instrument Contact Angle System OCA	Dataphysics, Filderstadt (GER)
Cooling Plate	Leica, Wetzlar (GER)
Digital Camera	Canon, Krefeld (GER)
Embedding Station	Thermo Fisher Scientific, Dreieich (GER)
Freezer: – 80 °C – 20 °C	 Kendro, Munchen (GER) Liebherr, Biberach a.d. Riss (GER)
Freezing Container: Mr. Frosty	VWR, Darmstadt (GER)
Glass slides	Superfrost plus, Thermo Scientific, (GER)
Ice Machine: „AF-80“	Scotsman, Mailand (ITA)
Immersion Thermostat for Water Bath	Lauda, Lauda-Konigshofen (GER)
Incubator	Medite, Burgdorf (GER)
Laboratory bottle: 1 l, 250 ml, 100 ml, 50 ml	Schott, Main (GER)
Laminar air flow cabinet Safe 2020	Thermo Fisher Scientific, Dreieich (GER)
Liquid Nitrogen Storage Tank: MVE 815 P-190 (–180 °C)	German-cryo, Juchen (GER)
Magnetic Stirrer with Integrated Heater Type 720-HPS	VWR, Darmstadt (GER)
Microplate Reader: Tecan Sunrise	Tecan, Crailsheim (GER)
Microscopes: Axiovert 40C AxioVision Observer.D1	 Zeiss, Göttingen (GER) Zeiss, Göttingen (GER)

FluorChem™ Q System Keyence BZ-9000 (Biorevo) Leica Confocal	ProteinSimple, Santa Clara (USA) KEYENCE Deutschland GmbH, Neu-Isenburg (GER) Leica, Wetzlar (GER)
Microsurgical Instruments	Fine Science Tools, Heidelberg (GER)
Multistep Pipette	Brand, Wertheim (GER)
Neubauer Cell Counting Chamber	Hartenstein, Wuerzburg (GER)
pH Meter	Mettler Toledo, Giessen (GER)
Pipettes: 0.5 – 10 µL, 10 – 100 µL, 100 – 1000 µL	Eppendorf, Hamburg (GER)
Pipetting Aid: Pipet Boy	Brand, Wertheim (GER)
Power Supply Model DES50PN-10 W	Gamma High Voltage, Ormond Beach, FL (USA)
Pump	Ismatec, Wertheim-Mondfeld (GER)
Pump tubing cassette	Ismatec, Wertheim-Mondfeld (GER)
Protective goggles	NeoLab, Heidelberg (GER)
Pressure measuring device	Chair Tissue Engineering and Regenerative Medicine, Wuerzburg, (GER)
Rocking Platform Shaker	NeoLab, Heidelberg (GER)
SEM: AURIGA 60	Carl Zeiss Microscopy, Oberkochen (GER)
Sliding microtome Leica SM 2010R Leica CM 1850UV	 Leica, Wetzlar (GER) Leica, Wetzlar (GER)
Steam Cooker: „MultiGourmet“	Braun, Kronberg/Taunus (GER)
Syringe Pump AL - 1000	World Precision Instruments, Sarasota, (USA)
Timer	Carl Roth GmbH, Karlsruhe (GER)
Ultrapure Water System	Millipore, Schwalbach (GER)
Universal Mechanical Test Machine, Zwick Z010	Zwick, Ulm (GER)

Vortexer	Carl Roth GmBH, Karlsruhe (GER)
Water Bath	Ulabo Labortechnik, Seelbach (GER)
Weighting machines: Analytical balance Precision balance	 Kern, Balingen–Frommern (GER) Kern, Balingen–Frommern (GER)

3.7. Disposable materials

Disposable materials are shown in Table 7.

Table 7. Disposable materials

Disposable materials	Manufacturer
Aluminum Foil	Carl Roth GmBH, Karlsruhe (GER)
Catheter 13 G, 18 G, 20 G, 22 G	B. Braun Melsungen AG, Melsungen (GER)
Cell Culture Flasks: 75 cm^2, 150 cm^2	TPP, Trasadingen (GER)
Cell Culture Multiwell Plates: 6 well, 12 well, 24 well, 96 well	TPP, Trasadingen (GER)
Centrifuge Tubes: 15 ml, 50 ml	Greiner Bio-One, Frickenhausen (GER)
Combitips Plus: 0.5 ml, 1 ml, 2.5 ml, 5 ml	Eppendorf, Hamburg (GER)
Cover Slips for Object Slides: 24 x 60 mm	Menzel-Glaser, Braunschweig (GER)
Cryo Tubes: 1.8 ml	Nunc, Wiesbaden (GER)
Dako Pen	Dako, Hamburg (GER)
Disposal Bags	Hartenstein, Wuerzburg (GER)
Disposable microtome blades, A35	Pfm medical, Cologne (GER)
Disposable Pipettes: 5 ml, 10 ml, 25 ml, 50 ml	Greiner Bio-One, Frickenhausen (GER)
Gloves: Latex Nitrile	 Cardinal Health, Kleve (GER) Kimberly-Clark, Koblenz (GER)

Object Slides: uncoated (26 x 76 x 1 mm) PolysineTM (25 x 75 x 1 mm)	 Menzel, Braunschweig (GER) Langenbrinck, Emmendingen (GER)
Parafilm R, M	Carl Roth, Karlsruhe (GER)
Pasteur Pipettes	Brand, Wertheim (GER)
Petri Dishes: 145 x 20 mm	Greiner Bio-One, Frickenhausen (GER)
Pipette Tips: 0.5 – 10 µL, 10 – 100 µL, 100 – 1000 µL	Eppendorf, Hamburg (GER)
Prolene suture	Ethicon, (USA)
Pump tubing	Ismatec, Wertheim-Mondfeld (GER)
Scalpel Blades, rounded	Bayha, Tuttlingen (GER)
Sterile Filter (Attachement for Disposable Syringes): Diameter 50 mm, Pore Size 0.2 µm	Sartorius Stedium Biotech, Goettingen (GER)
Syringes: 5 ml, 10 ml, 20 ml, 50 ml	BD Biosciences, Heidelberg (GER)
Weighing Dish	Hartenstein, Wuerzburg (GER)

3.8. Software

Used software is listed in Table 8.

Table 8. Software

Software	Manufacturer
Image J	Wayne Rasband, NIH (USA)
Keyence BZ-II Viewer Keyence BZ-II Analyzer	KEYENCE Deutschland GmbH, Neu-Isenburg (GER)
Office Word 2010 Office Excel 2010 Office PowerPoint 2010	Microsoft Deutschland GmbH, Unterschleißheim (GER)
Pressure control	Tissue Engineering and Regenerative Medicine, Würzburg (GER)
Tecan i-control™ 1.7	Tecan, Crailsheim (GER)

4. Methods

4.1. Incubation conditions

The entire cell culture work was performed under sterile conditions in a safety cabinet – sterile bench. Morphology was examined daily via light microscopy. All cells were cultured under standard culture conditions i.e. at 37 °C, under an atmosphere of 5 % CO_2 and 95 % humidity. The medium was refreshed 2 – 3 times a week using VascuLife® medium, which had been pre-warmed at 37 °C for 10 – 15 min before use.

4.2. Isolation and culture of primary endothelial cells

Primary endothelial cells were isolated from fresh biopsies. The procedure was approved by the ethical commission of the University of Wuerzburg (vote 182/10). Human prepuce was used, which was stored for a maximum of 24 hours at 4 °C in transport medium (Table 3). To prevent a cellular cold shock, the medium and all solutions were heated up to 37 °C in a water bath before they were used.

At first, the biopsy was washed three times with a phosphate buffered saline solution without calcium chloride and magnesium chloride (PBS^-) in a 90-mm petri dish in order to remove the transport medium dead cells and debris. Following, the subcutis was removed with a sterile scalpel and washed again three times with PBS^-. In the next step, the biopsy was cut into 2-mm-thin stripes. These stripes were washed three times with PBS^-. The petri dish was then filled with a dispase solution (4 U/ml in PBS^-) until the stripes were covered. After sealing the petri dish by using parafilm, it was incubated 16 to 18 hours at 4 °C. The next day, two petri dishes with PBS^- were prepared. Then, the epidermis and the dermis were separated, using two sterile tweezers and placed into one petri dish each. If the layers couldn't be separated, the whole petri dish was placed in the incubator (5 % CO_2, 37 °C, 95 % RH) until separation was possible. After successful removal of the epidermis, the dermis was washed with a solution of 0.1 vol-% Ethylenediaminetetraacetate in PBS^- (PBS^- /EDTA) and then covered with 10 ml of a 0.05 vol-% trypsin in PBS^-/EDTA solution (trypsin/EDTA). EDTA is used as a chelating agent that binds calcium and prevents joining of cadherins between cells. (55) If EDTA is present, cell-cell-bindings are released. Trypsin is a mix of different enzymes, which cuts lysine, arginine and modified cysteine in proteins. (56) Incubating cells with trypsin

detaches the cells from a surface e.g. of the cell culture flask. The dermis was incubated for 40 min in the incubator and then trypsin activity was stopped adding 25 vol-% fetal calf serum (FCS). After that, the stripes were placed into another petri dish filled with VascuLife® and were crossed out ten times each side using a sterile scalpel with gentle pressure. To free the cell suspension from smaller tissue parts, the cell suspension was filtered through a cell strainer with 100 µm pore size into a 50 ml Falcon tube. To increase the harvest, the petri dish was washed three times with 5 ml VascuLife®. Then, the suspension was centrifuged for 5 min at 1200 rpm.

After discarding the liquid, the pellet was resuspended in 2 ml VascuLife®. Finally, the cells were counted using a Neubauer counting chamber. Therefore, 20 µl of the cell suspension were mixed with 20 µl trypan blue in a 96-well plate and subsequently filled in the counting chamber. Living and dead cells could be distinguished by staining: living appeared colorless whereas dead cells were colored in blue. The mean number of living cells was determined using Equation 1. The number of the counted cells was divided by 4 because of the four squares of the counting chamber. Then, the result was multiplied by 10,000 to get the number of cells per 1 ml. Finally, the result was multiplied by 2 because the cells were mixed with trypan blue in a ratio of 1:2 prior to counting.

Cell number could be determined as follows:

$$MeanLC * 10^4 * 2 = living\ cells/ml \qquad (Equation\ 1)$$

MeanLC: mean of living cells per quadrant

Cells were seeded into the cell culture flasks (1.2 x 10^4 cells/cm^2). 3 ml VascuLife® per 25 cm^2 and 1 vol-% of the antibiotics penicillin and streptomycin (pen/strep) were added to the flasks. After seeding the flasks, they were placed in the incubator.

4.3. Passaging cells

HmvEC were passaged once a week at a confluence of 70 – 90 %. At first, the medium was aspirated, and cells were washed with PBS^-/EDTA to remove remnants of the serum.

Cells were then incubated with 0.1 % Trypsin/EDTA solution at 37 °C for 3 min. The detachment of the cells was confirmed by microscopy. Trypsin reaction was stopped by adding FCS. Via pipetting the suspension up and down several times, remaining cell clusters were disrupted for a single cell suspension, which was then transferred to a 50-ml centrifuge tube. The suspension was centrifuged at 1200 rpm for 5 min and after that the supernatant was aspirated. After resuspending the cells in fresh medium and counting the cells, they were reseeded at their respective densities. Cell lines were used until passage 4.

4.4. Determination of cell number and vitality

Cell number and vitality was determined using trypan blue staining. Therefore, an aliquot of the cell suspension was mixed 1:2 with 0.4 % trypan blue solution. 10 µl of this mixture were pipetted into a Neubauer counting chamber and cells were counted in all four quadrants under the microscope. Living cells appeared colorless whereas dead cells were colored in blue, as described in 4.2. Cell vitality could be determined as the quotient of living cell number to total cell count, and was generally indicated as percentage.

4.5. Freezing and thawing of cells

To preserve cell stocks in a low passage number, cells were cryopreserved at 10^6/ml cells in cryo tubes. After expansion, cells were detached from the culture flask as described in 4.3, and cell number was determined as described in 4.4. HmvECs were stored in VascuLife® medium (concentration 10^6 cells/ml) with addition of 10 % (v/v) FCS as well as 10 % (v/v) DMSO (dimethyl sulfoxide). This cell suspension was distributed to cryo-tubes at 1 ml per tube and inserted into the "Mr. Frosty" freezing container. "Mr. Frosty" was then placed in – 80°C freezer for at least 24 h, to assure a slow freezing process of – 1 °C per minute to avoid formation of ice crystals. After that for a long-term storage liquid nitrogen tank was used.

To thaw cells, cells were shortly placed in warmed 37 °C water bath until a small piece of ice remained, after taking the cryo tubes out of the liquid nitrogen tank. The cell suspension was then immediately transferred to a 50-ml centrifuge tube containing 9 ml of pre-warmed cell-specific medium (VascuLife®) and centrifuged for 5 min at 1200 rpm. The supernatant was aspirated, and the cell pellet was resuspended in 6 – 9 ml fresh pre-

warmed VascuLife® medium and added to a cell culture flask. Next day, the VascuLife® was changed. Thawed cells were passaged at least once before they were used for experiments.

4.6. Magnetic activated cell sorting – MACS of hmvEC

To achieve highly pure endothelial cell culture from foreskin tissue, Magnetic Activated Cell Sorting (MACS) was performed using CD31 MicroBead Kit (Miltenyi Biotec GmbH, Germany), before the use of cells in in vitro experiments. After treatment of the cultured cells with trypsin, $CD31^+$ hmvEC were immunolabeled with CD31 MicroBeads, before being loaded onto a column placed in the magnetic field of a MACS Separator. The magnetically labeled $CD31^+$ cells were retained within the column. The unlabeled cells ran through the column and were later discarded. After removing the column from the magnetic field, the magnetically retained $CD31^+$ cells could be eluted as the positively selected cell fraction and directly taken into further hmvEC pure cell culture as shown on Figure 6.

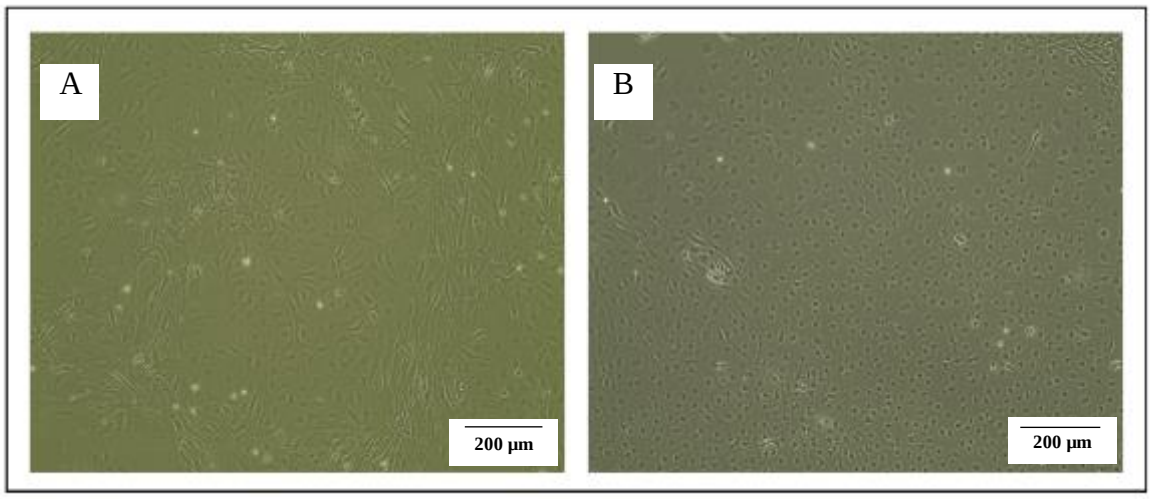

Figure 6. Microscopy of human microvascular endothelial cells (hmvECs)*. Images show hmvECs mixed with fibroblasts in cell culture before (A) and after MACS Sorting(B).*

4.7. Isolation of collagen type I from rat tails

For the isolation of collagen type I, rat tails were incubated for 2 min in 70 % (v/v) EtOH. Afterwards, the skin of rat tails was stripped. After washing in PBS^-, the tendons were excerpted and washed three times with PBS^-. For disinfection, tendons were washed twice with 70 % (v/v) EtOH followed by three washing steps in PBS^-. After weight measurement, tendons were incubated in 0.1 % (v/v) acetic acid in a spinner flask under constant agitation at 4 °C for two to three weeks until no tendon leavings or transparent clumps were visible. Then, collagen solution was centrifuged at 7,700 rpm for 1 h at 4 °C. Collagen solution was mixed for 20 min and collagen content was determined to obtain a concentration of 10 mg/ml collagen type I dissolved in 0.1 % (v/v) acetic acid. The whole process of collagen isolation was kindly performed by the Working Group Standardized in-vitro-test systems, Dr. Florian Groeber, Chair for tissue engineering & regenerative medicine.

4.8. Electrospinning process

Electrospinning represents a process in which a strong electric field is generated between a polymer solution (delivered through a syringe needle) and a metallic collector. Due to the applied voltage, the charge overcomes the surface tension of the polymer solution and

Figure 7. Electrospinning setting. *CAD-Design of electro-spinner render with SOLIDWORKS (kindly provided by Thomas Schwarz) and photograph of constructed electro-spinner.*

a drop at the needle tip is generated. Furthermore, a polymer jet develops and moves toward the collector. While traveling towards the metallic roller, the electric field forces the drawing of the drop. Simultaneously, solvent evaporates. This results in reduction in the diameter of the jet and the drawn polymer in solid state is deposited on the collector. The collected dry fibers form a mesh of fibers ranging from nanometer to micrometer diameter sizes. The whole process can be adjusted to that extent to control the diameter of fibers by varying the charge density and polymer solution concentration.

Tissue scaffolds were fabricated by electrospinning of PCL and collagen type I, which were separately dissolved. PCL was dissolved in 1,1,1,3,3,3-Hexafluoro-2-propanol (HFIP) at the concentration of 15 % (w/v) and isolated collagen type I, after lyophilisation, was dissolved in trifluoroethanol (TFE) at the concentration of 5% (w/v). A modified bi-directional gradient electrospinning system was developed in the Chair for tissue engineering & regenerative medicine as showed in Figure 7. It consists of:

- Two pumps
- Rotating collector
- Power supply
- Closed chamber
- Control panel
- Vent-hole

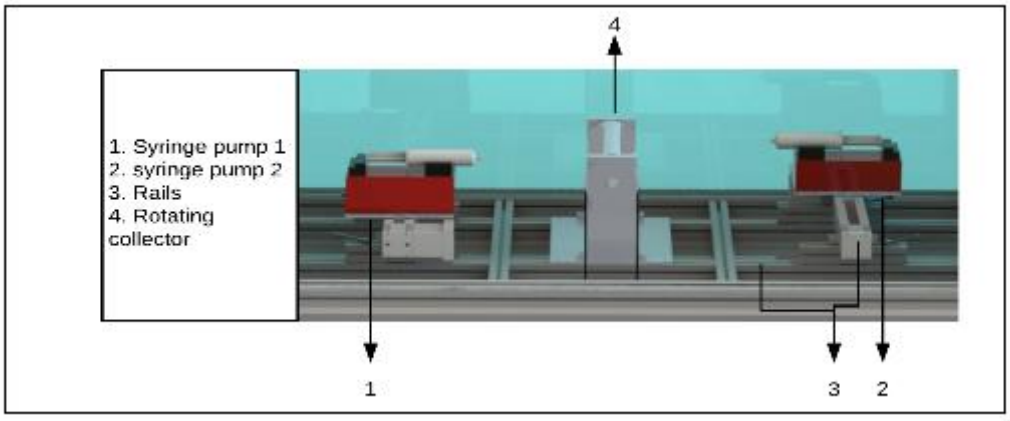

Figure 8. Electrospinning setting – detailed. *CAD-Design of 2 syringe pumps and rotating collector inside the electrospinner. Both pumps are placed on rails providing the movements in x and z axis, allowing modification of pump-collector distance. Kindly provided by Thomas Schwarz*

The electrospinning setting included two syringe pumps, a high-voltage supply, and a rotating mandrel (Figure 8). A positive voltage (8 – 15 kV) was applied to the polymer solutions. The two syringe pumps were used to pump polymer solutions in opposite directions toward the rotating mandrel. A stainless-steel mandrel (6 mm in diameter) with rotation speed ranging between 0.162 – 0.315 m/s was used to collect scaffolds. The distance between each syringe tip and the mandrel was 10 cm. To fabricate multi-layered scaffold with gradient symmetrical structure, continuous bi-directional electrospinning was applied with the gradually increasing and decreasing flow rates (mL/h) of collagen type 1 to PCL as showed on Table 9.

Table 9. Polymer flow rate changes during the electrospinning process

PCL flow (ml/h)	Collagen type I flow (ml/h)	Duration (min)
0	0.4	30
0.2	0.4	15
0.4	0.2	15
0.6	0	60
0.4	0.2	15
0.2	0.4	15
0	0.4	30

For testing the scaffolds antibacterial activity in vitro, we produced scaffolds with addition of antibiotics (vancomycin hydrochloride and gentamicin sulfate) into core PCL layer. The core layer is the middle layer of multilayered scaffold and consists only of PCL nanofibers. Therefore, we prepared collagen I as described, and for the core layer PCL, vancomycin and gentamicin (15% : 6% : 1% w/v) was dissolved in 1,1,1,3,3,3-hexafluoro-2-propanol (HFIP). The further electrospinning process was performed as described previously.

During the electrospinning process, the temperature in electrospinning chamber was stabile 22 ^{o}C and relative humidity between 25 – 29 %.

4.9. Crosslinking of collagen scaffolds

After electrospinning, all collagen containing scaffolds were crosslinked before seeding with microvascular endothelial cells. The crosslinking was performed using 10 % hexamethylen-diisocyanat (HDMI) for up to 1 h. Subsequently, scaffolds were washed 3x with 100 % Isopropanol for 20 min, and then rinsed 3x in 70 % Ethanol under a sterile bench. As the last step, scaffolds were washed 3x in PBS^- solution for 10 min. All scaffolds were sterilized using gamma-radiation and stored under sterile conditions. Before cell seeding, all scaffolds were rinsed in PBS^- solution.

4.10. Mechanical properties

Tensile mechanical property

Tensile mechanical tests of all scaffolds were performed using a universal material testing machine Zwick at the ambient temperature and humidity. All samples were prepared in the same size of 50 mm x 5 mm. A cross-head speed of 10 mm/min was used for all the specimens tested until failure. The test was aligned to the American Society for Testing and Materials (ASTM) guideline D 882-02 (Standard Test Method for Tensile Properties of Thin Plastic Sheeting).

Burst pressure

For burst pressure measurement, a 3-cm-long and 5-mm-thick glass tube was connected to a pressure recording device (Chair Tissue Engineering and Regenerative Medicine, Wuerzburg, Germany) on one side. The opposite side was hermetically sealed with an electrospun vascular scaffold using suture threads. A manual filling with water was applied and the filling pressure was recorded until the scaffold wall failed. The maximum recorded pressure was set as burst pressure of the graft. All measurements were repeated on 4 samples for each type of vascular scaffold.

Suture retention strength

Suture retention strength was measured with a tensile testing machine equipped with a 200-N-load cell. To determine the suture retention strength, the vascular graft was cut normal to the long axis into small strips dimension of 20 mm x 5 mm. On one end, electrospun vascular scaffolds were clamped and on the other, 5±0 prolene suture was

passed through it and knotted at distance of 2 mm from the scaffold edge. The suture was pulled at a rate of 50 mm/min. The force required to pull the suture through the graft wall was recorded as suture retention strength. This test was repeated on 3 samples for each type of vascular scaffold.

Wettability

Surface wettability of different scaffolds was tested by measuring angle of water droplets by using contact angle measuring instrument. Two different positions on 6 samples of each scaffold were tested, and 0.02 mL deionized water was used for each measurement.

4.11. Seeding the cells on electrospun matrices

Preparation and culture of cell crowns

Sterilized electrospun scaffolds were placed in petri dish and washed with PBS^- solution. Each matrix was cut using sterile scalpel and tweezers in approximately 1 cm^2 pieces. These were then placed onto the inner ring of metal cell crown, regardless of which side is pointing upwards as shown in Figure 9. Following, the outer ring of cell crown was fixed onto the inner ring. The cell crown was then turned downside up and placed into a 12-well plate with crown spikes pointed down.

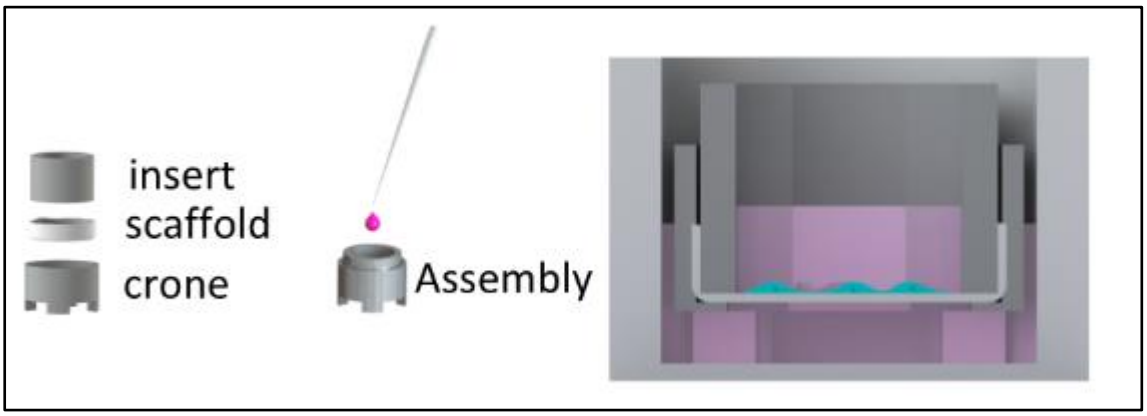

Figure 9. Process of fixation of scaffolds into cell crowns and cell seeding. *The scaffold is first placed between two part of cell crown, then are the hmvECs added. hmvECs arrangement inside the cell crown is showed on the right side. Kindly provided by Thomas Schwarz. (Also used for publication in PLoS ONE (1))*

For seeding the cell crowns, the cells were detached as described in 4.3, followed by cell counting as described 4.4. All cell crowns were filled with up to 1 mL Vasculife® and placed in incubator for 1 hour. Afterwards, medium was aspirated out of each cell crown, and then seeded with the $4x10^5$ hmvEC onto the inner part of the cell crown. The inner part was filled up to 1 mL with Vasculife® (already containing 1 % Pen/Strep) and the outer part with 1.5 mL Vasculife® so that the liquid level was the same on the inner and outer side of the cell crown in each well. For further static cultivation, plates were placed in an incubator (37 °C, 5 % CO_2, 95 % rH). The culture medium (Vasculife®) was replenished every 2 days. The schematic process of preparation of cell crowns is shown in Figure 9. Such a setting provides also a possibility of growing the same or different cell type on the other side of the scaffold, which in this study was not needed.

Preparation of bioreactors and dynamic cell culture

For dynamic cell culture tests, electrospun tubes – 6 mm in diameter (Figure 10A), were then crosslinked as described, and the sterilization was performed using Gamma radiation. After Gamma sterilization, the bioreactor setup in which hmvECs were seeded into scaffolds luminal side was prepared. This was done under sterile bench and in sterile conditions. The bioreactor chamber in which the graft for cell seeding was placed was custom made. Therefore, parts of two 15 mL Falcon tubes were combined with, silicone hoses and silicon glue as shown in Figure 10. The concept was kindly provided by Sebastian Schürlein. The prepared graft scaffold made of PCL and collagen type I is first clamped inside the bioreactor under sterile conditions and made tight to connectors using ligature suture. Afterwards, a sterilized silicone tube bigger in diameter than the inner tube was pulled over to seal the bioreactor. Thereby, an extra luminal compartment was generated. The bioreactor system enabled distinct extra and intra luminal flow conditions. At the in- and out-let of the bioreactor, a three-way valve was attached to enable controlled filling of the graft with cell containing medium. The cells were detached as described in 4.3, followed with cell counting as described in 4.4. Approximately $4x10^6$

hmvEC were used for a 4-cm-long graft. Each graft, already clamped in bioreactor, was first filled with Vasculife® and incubated in incubator for 1 h.

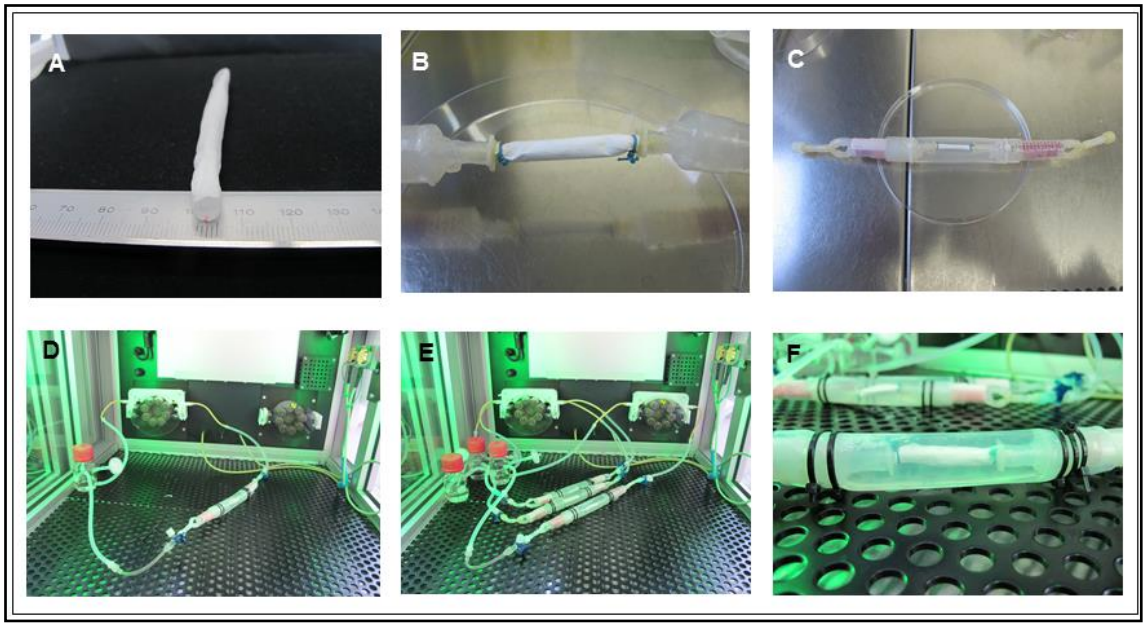

Figure 10. Bioreactor setup. *Here is shown how are scaffolds prepared for cell seeding after electrospinning (A). First the scaffold is clamped between two connectors using ligature (B), silicone hose is then pulled over scaffold to build outer medium chamber (C). After filling with hmvECs and incubation in static incubator for up to 4 hours the whole system is prepared for dynamic cultivation (D-F)*

Afterwards, grafts were filled, only the inside lumen, with new medium containing already stated cell count and then incubated in the incubator (37 °C, 5 % CO_2, 95 % rH) for 4 hours. For filling the bioreactor, sterile 5 mL syringes were used. Every 30 min, the whole bioreactor was rolled for 180° allowing gradual attaching of the hmvEC onto all sides of inner lumen of the graft. Subsequently, the bioreactor was to connect with all parts of previously described bioreactor system, to fill the whole system with pre-warmed culture medium, Vasculife® with 1 % Pen/Strep, filling also the reservoir with up to 30 mL. Finally, the whole bioreactor system was placed in incubator with ISMATEC® pump running constant pumping speed of 4 rpm flow rate. Both chambers of the bioreactor were exposed to medium flow. The medium in whole system was changed once a week.

The whole bioreactor system and incubator chamber for dynamic cultivation was made from several parts as shown in Figure 11. It consists of small 50 mL glass bottle (**1)** with a filter on the air side. This bottle operates as the reservoir for the medium and it is connected to the pump (**2)**. This roller pump is providing constant medium circulation from the reservoir to the bioreactor and back into the medium reservoir. The ISMATEC® pump is set to a constant pumping speed of 3.2 mL/min (4 rpm). To the incubator chamber is connected a CO_2 inflow (3) and inside the chamber is CO_2 sensor, which continuously monitors its concentration inside the chamber. A heating plate (**5**) is used to keep the temperature inside the incubator constant. All parts of this bioreactor system are connected with electrospun graft (6) using silicone tubes.

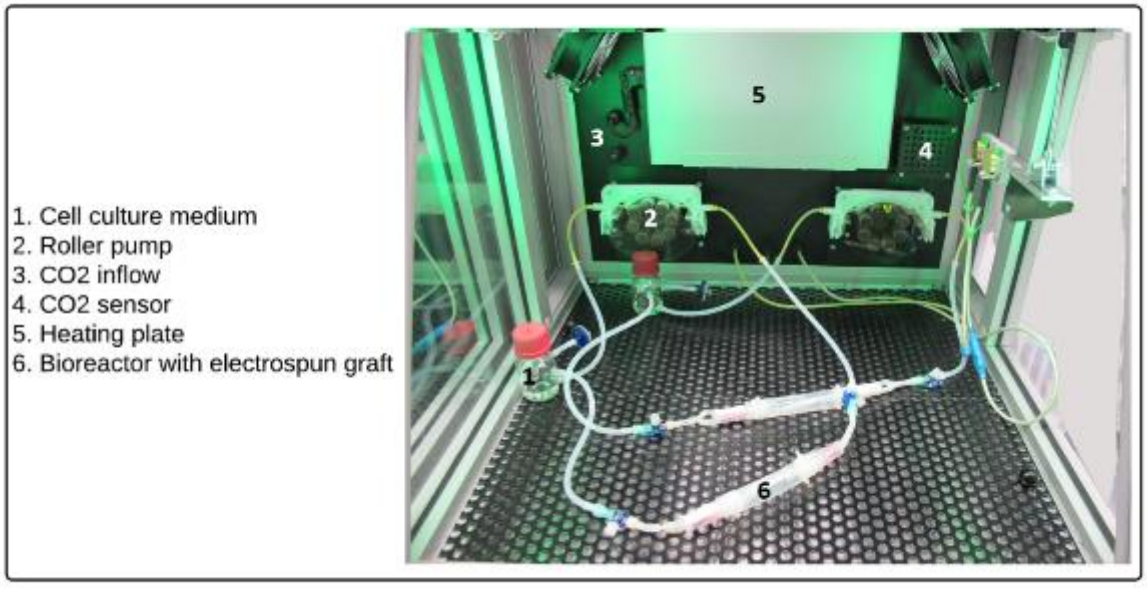

Figure 11. Dynamic flow bioreactor setting

4.12. Histology and immunohistology

Preparation of frozen tissue sections

To perform histological or immunofluorescence staining, all matrices and grafts were after incubation first fixed in 4 % PFA at room temperature. After 1 h, the PFA was aspired and the inserts were washed with PBS^-. Afterwards, inserts or graft samples,

which were cut with scalpel, were placed into special tissue embedding cassette and covered with cryo-embedding media (Tissue-Tek, O.C.T., Sakura, The Netherlands), and placed on a dry ice to freeze. After the tissue block was completely frozen, it was stored at – 80 ^{o}C until ready for sectioning. Section was performed in cryotome cryostat at – 20 ^{o}C (Leica CM1860, Leica Biosystems, Germany) after allowing the temperature of the frozen tissue block to equilibrate to the temperature of the cryotome cryostat. The frozen tissue block was then cut into 5 µm thick sections and sections were placed onto glass slides, and dried overnight. The slides were then used for further histological and immunohistochemical staining.

Hematoxylin and eosin staining

HE staining was performed to provide an overview of the tissue morphology. The treatment of the slides with frozen insert slices was performed as described in Table 10.

Table 10. Staining protocol for Hematoxylin and eosin staining (HE)

Time in min	Solution	Notes
Swirl until no turbulences	VE water	Rehydration
6	Hemalaun	Staining of cell nuclei
5	Running tap water	Coloring hemalaun
6	Eosin	Matrix and cytoplasm staining
Until no color washes out	VE water	Washing
Dip 3 times	70% ethanol	Dehydration
2	96% ethanol	Dehydration
5	Isopropyl alcohol I	Dehydration
5	Isopropanol alcohol II	Dehydration

The hemalum stained basophilic structures such as cell nuclei in blue. Eosin counterstained acidophilic structures red and pink. Tissue sections were mounted with Entellan mounting medium and cover slips for preservation.

Immunofluorescence

Immunofluorescence staining was performed to stain components or markers in the electrospun matrices or vascular grafts. Although the staining procedure varies slightly, the basic concept is the same: A primary antibody of either rabbit or mouse origin acts against a target protein. In a consecutive incubation, a secondary antibody from a different host than target cell and primary antibody, binds to the primary antibody and carries a fluorochrome, which then can be excited in the fluorescence microscope and emits light of a certain wavelength. All staining steps starting from the sec. antibody incubation had to be performed in the dark, as those fluorochromes are very photosensitive. Cover slips were mounted on the samples using Mowiol with 4',6-Diamin-2-phenylindol (DAPI) which stains the cell nuclei blue. The successive staining procedure was performed as shown in Table 11.

Table 11. The immunofluorescence staining procedure

Solution/Procedure	Time in min.
VE water	Swirl until no turbulences
Washing buffer	3 x 5
Cooked in citrate buffer pH 6.0 (90-100 °C)	20
Washing buffer	3 x 5
Hyaluronidase ($300mg^{-1}$)	15, at 37°C
Washing buffer	3 x 5
Blocking serum 5%	20
Primary antibody	Over night, 4°C
Washing buffer	3 x 5
Secondary antibody	60, keep dark
Washing buffer	3 x 5, keep dark
MOWIOL DABCO with 0,1 % DAPI	Mount and add cover slip

Washing buffer - PBS^- with 0.5 vol-% tween-20

Stained samples were left to dry overnight and had to be stored kept away from light.

4.13. Cell viability measurement

3-(4,5-dimethyl-2-thiazolyl)-2,5-diphenyl-2H-tetrazolium bromide (MTT) Assay was performed to assess cell viability macroscopically by detection of viable cells seeded on

electrospun scaffolds. The MTT assay is based on the reduction of tetrazolium dye MTT to blue in soluble formazan by cellular enzymes of metabolically active cells. All samples were transferred in 12-well plates and incubated in MTT reagent (1 mg/mL in cell culture medium) for 90 min. Following, qualitative and quantitative analyze were performed. After washing with PBS^-, samples were photographed and documented. To quantitatively evaluate cell viability and to compare different scaffolds, acid isopropanol (100 µL of 0.04 N HCL) was added to wells and mixed thoroughly to dissolve dark blue crystals. After a few minutes at room temperature to ensure that all crystals were dissolved, 200 µL was added to 96-well plates and the plates were read on a Tecan infinite M200 reader, using a test wavelength of 570 nm, a reference wavelength of 630 nm, and a calibration setting of 1.99 (or 1.00 if the samples were strongly colored). Plates were analyzed within 1 hours of adding the isopropanol.

4.14. Determination of acetylated low-density lipoprotein

AcLDL test was performed to metabolically label endothelial cells using acetylated-low density lipoprotein (acLDL), which is taken up by endothelial cells via the "scavenger cell pathway". For this test the tissue was placed in 12-well plate filled with Vasculife® medium. Next, the acLDL, which is fluorescently labeled with Alexa Fluor 488 (by Life technologies), was add to cell medium to achieve concentration of 10 µg/mL. Also 10 µL/mL of Hoechst (by Life technologies) was added to cell medium to stain the cell nuclei. Following, plates were placed in incubator for 2 hours, and after being thoroughly washed with PBS^-, tissue samples were analyzed under a confocal microscope (Leica).

4.15. Cell vitality and scaffold cytotoxicity assay

A Live/Dead Assay is suitable for determination of live and dead cells after seeding and incubation on scaffolds. In our study, the test was based on intracellular esterase activity of living cells and plasma membrane disintegration of dead cells. All samples were put in 12-well plates and few drops of Live/Dead solution were added. Live/Dead solution consists of fluoresceindiacetat (FDA) staining that only visualizes the living cells, and propiumbromiodide (PI) staining only dead cells. The solution was prepared by adding 1 µL of FDA and 9 µL PI into 990 µL PBS^-. After allowing it to soak on the scaffolds,

samples were washed with PBS^- and examined immediately under the fluorescence microscope.

4.16. The antibacterial efficacy of electrospun grafts containing vancomycin/gentamicin in vitro

As experimental bacterial strain *Staphylococcus aureus* and *Staphylococcus epidermidis* were. Staphylococci are the most common microorganisms that can cause implant-related infections. The S*taphylococcus aureus* strain (DSM-799 from DSMZ - German Collection of Microorganisms and Cell Cultures) and *Staphylococcus epidermidis* (O-47 from The Institute for Molecular Infection Biology, University Wuerzburg) were used to inoculate a Mueller-Hinton (MH) plate uniformly. To carry out a bacterial inhibition test, we used our standard PCL/collagen matrices on the one side and the same triple layer matrices with PCL/antibiotics combination for the core layer. The process of electrospinning was described before in 4.8. Each matrix was cut in circle samples representing 6 mm disc. The discs were placed on nutrient agar plates and seeded with a layer of a *Staphylococcus aureus* or *Staphylococcus epidermidis* respectively. The agar plates were incubated at 37 °C and analyzed at 24-h intervals. The zones of inhibition were photographed with digital camera and measured with a micrometer.

4.17. Scanning electron microscopy

To characterize the morphology, size and orientation of the fibers of electrospun matrices scanning electron microscopy was performed. The coating procedure was performed using platinum, and the SEM analyses were kindly performed by Tobias Weigel in Fraunhofer ISC in Würzburg. Fiber diameter and pore size measurements were performed using ImageJ software.

4.18. Statistical analysis

All quantitative results were obtained from triplicate samples. Data were expressed as mean ± standard deviation (SD). Data was analyzed on normal distribution using the Kolmogorov-Smirnov-Test. Statistical analysis was performed using an unpaired student's t-test and ANOVA analysis of variance. A p-value of $p < 0.05$ was considered as statistically significant.

5. Results

5.1. Morphology and biomechanical properties of nanofibrils scaffold

In this study, a multi-layered porous nanofibrils scaffold was generated by sequential electrospinning of two solutions with different polymers composed of PCL and collagen type I. During the electrospinning process, controlled temperature and humidity conditions were ensured. Additionally, grafts of pure PCL were fabricated as reference. For preparing multi-layered PCL/collagen tubular scaffold (Figure 10A), the luminal layer was first fabricated by spinning of collagen type I. Following, bidirectional gradient spinning was performed by simultaneously increasing or decreasing the flow rate of PCL and collagen type I, respectively as shown in Table 9.

Structural characterization

By controlling the flow rates, the luminal and adventitial surface of multilayered scaffolds were composed of pure natural material – collagen type I. The introduction of transitional layer composed of both PCL and collagen, the susceptibility of delamination is reduced. Figure 12 shows SEM images of morphology of multilayered and pure PCL scaffolds. It displays the morphological change of nanofibers when using increasing concentration of PCL solution. In this experiment, the fabricated PCL and multilayered PCL/collagen vascular scaffolds exhibited fibrous structures (Figure 12A-F). Moreover, the addition of collagen type I resulted in an increase of the fiber thickness. The evaluation of the mesh porosity of 3 individual samples of each scaffold revealed maximum pore sizes of 10.66 μm^2 for 10 % PCL, 51.10 μm^2 for 15 % PCL, and 54.34 μm^2 for 20 % PCL scaffolds. For the multilayered electrospun scaffolds, a robust measurement of the pore size was not applicable due to the formation of merged fiber structures. Nevertheless, crosslinking of collagen type I resulted in smaller pore sizes in the collagen/PCL scaffolds compared to PCL structures.

Surface wettability of material has a significant effect on cell adhesion, proliferation and migration. At the lower right corner in the images in Figure 12, the wettability of the respective scaffold is depicted. Pure PCL vascular grafts exhibited higher hydrophobic properties than multilayered vascular grafts with an average water contact angle of 130.3° ± 2.1°, whereas hydrophilicity of collagen-blended vascular grafts increased significantly

with an average contact angle of 102.1° ± 1.7°, as the surface of multilayered vascular grafts consisted of collagen type I (Inset in Figure 12A-F).

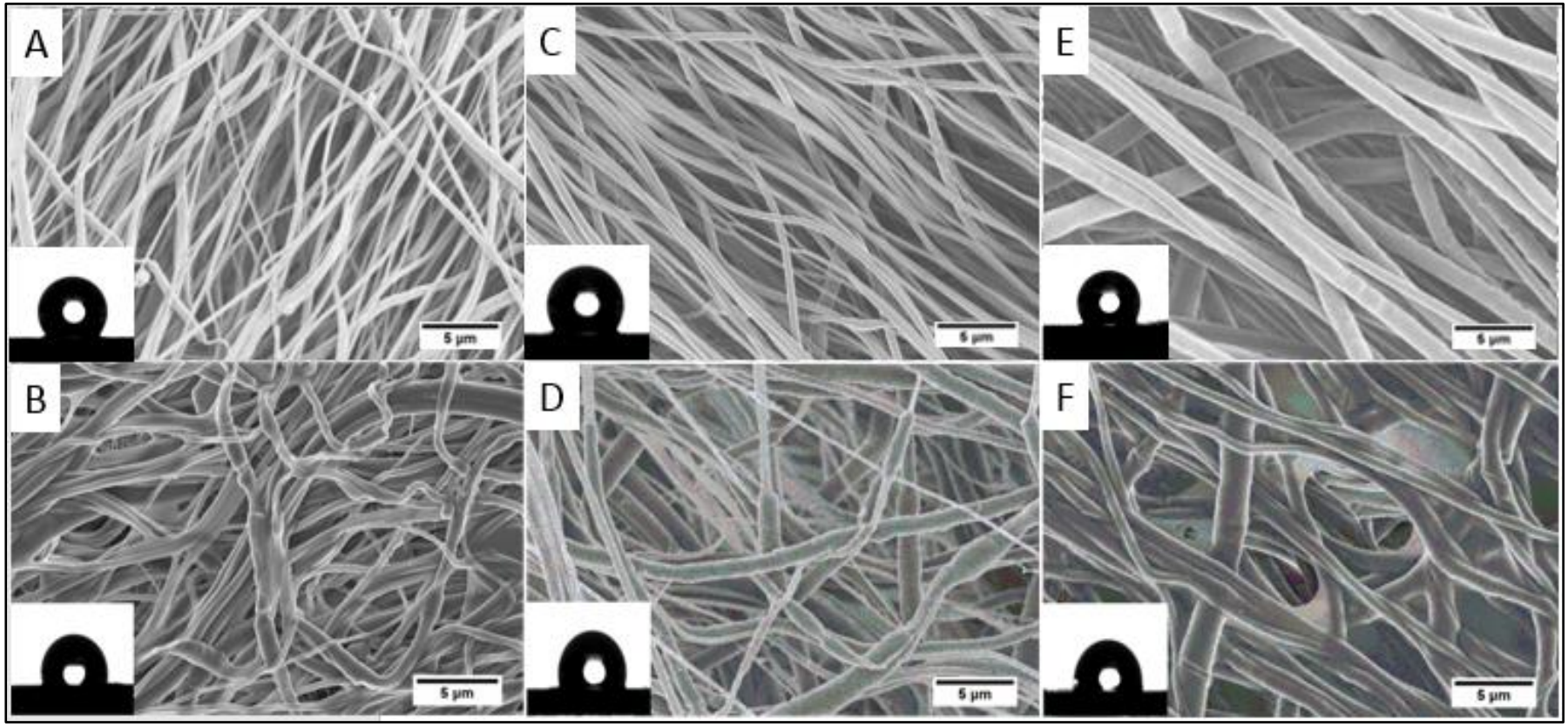

Figure 12. SEM images of different scaffolds and wettability. *On the images (A),(C) and (E) are shown PCL scaffolds made of 10 % (A), 15 % (C) and 20 % (E) PCL respectively. Images (B), (D), and (F) show scaffolds with same PCL concentrations which contain 5 % collagen type I on the inner and outer scaffold side 10 % (B), 15 % (D) and 20 % (F). In the left lower corner of each image is shown result of wettability test for each scaffold. (Also used for publication in PLoS ONE) (1)*

Mechanical characterization

After implantation, the grafts are part of arterial circulatory system with arterial blood pressure and must endure high mechanical forces in vivo. Thus, the mechanical properties of the scaffolds are a crucial parameter determining the success the graft.

To assess the mechanical properties, electrospun scaffolds were subjected to uniaxial elongation, in order to evaluate tensile strength and elasticity. Furthermore, suture retention and burst pressure test were performed to assess the scaffolds usability in clinical setting (Figure 13A-B). When comparing the mechanical properties of the different scaffolds, no impact of the PCL concentration on the young's modulus was found (Figure 13A). Compared to the PCL scaffolds, the multilayered scaffolds showed a decreased young's modulus. For 10 % and 15 % PCL, the reduction was statistically significant. In contrast to the young's modulus, the maximum elongation was significantly increased with increasing PCL concentration (Figure 13B). This effect was weakened for the multilayered grafts. Uniaxial tensile tests showed that the vascular grafts have an initial elastic behavior, followed by stiffening. This characteristic is similar to native arteries (57). The PCL vascular scaffolds revealed a superior tensile strength and higher maximum elongation compared to multilayered PCL/collagen scaffolds (Figure 13B). In analogy to the maximum elongation, also the suture retention strength was depended on the PCL concentration. Hereby, the highest suture retention strength of PCL scaffolds was found for a concentration 15 % PCL (Figure 13C). The suture retention strength of 15 % PCL and multilayered vascular graft (15 % PCL and collagen type I) was 1.62 ± 0.05 N and 0.43 ± 0.8 N, respectively (Figure 13C). Suture retention strength for PCL scaffolds were comparable to results previously reported and comparable to the suture retention strength of a saphenous vein. Multilayered vascular scaffolds showed lower suture retention compared to the results of native arteries reported by other investigators. (58) For the burst pressure, neither a dependency on the PCL concentration nor on the scaffold structure was found (Figure 13D). Burst pressure test showed that the maximal

burst pressure strength for multilayered vascular grafts consisting of 15% PCL and collagen type I was 664 mmHg (Figure 13D).

5.2. Cell seeding efficiency, viability and phenotypic expressions (cell crowns)

After fabrication of multilayered PCL/collagen and pure PCL scaffolds, those were placed in a cell crowns and seeded with the same amount of hmvEC as described in 4.11. and shown in Figure 9. After incubation period of one week, scaffolds were examined and cell seeding efficiency and viability were assessed.

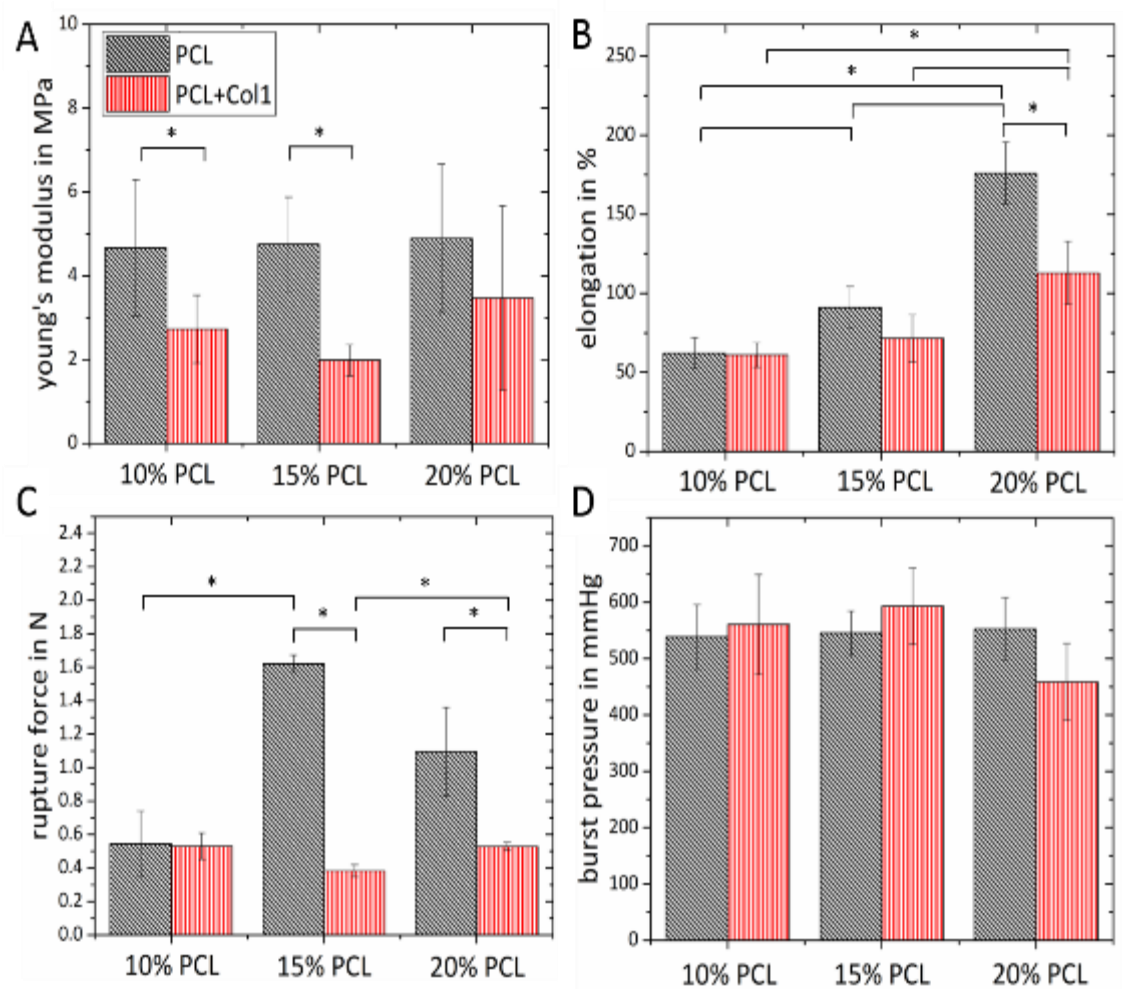

Figure 13. Mechanical properties of scaffolds*. Comparison of the mechanical properties of electrospun scaffolds produced from different PCL concentrations. (A) Young's modulus (n = 3), (B) maximum elongation (n = 3), (C) suture retention strength (n = 3), and (D) burst pressure (n = 4). Data are expressed as mean ± standard deviation (SD), * indicates significant differences (p-value < 0.05). (Also used for publication in PLoS ONE (1))*

In the H&E staining shown in Figure 14, a cell layer on all scaffolds was detected. Cells cultured on multilayered scaffolds tended to organize closer compared to pure PCL scaffolds, where regions without cells can be noted. When A 20 % PCL concentration resulted in a cell organization similar to multilayered scaffolds most probably due to bigger fiber size and smaller pore size preventing the hmvECs to fall through the scaffold during incubation and more surface to adhere. Moreover, it was possible to see how endothelial cells tend to organize in one layer during static cultivation in cell crowns as well on multilayered scaffolds when seeded on collagen side, as on pure PCL scaffolds.

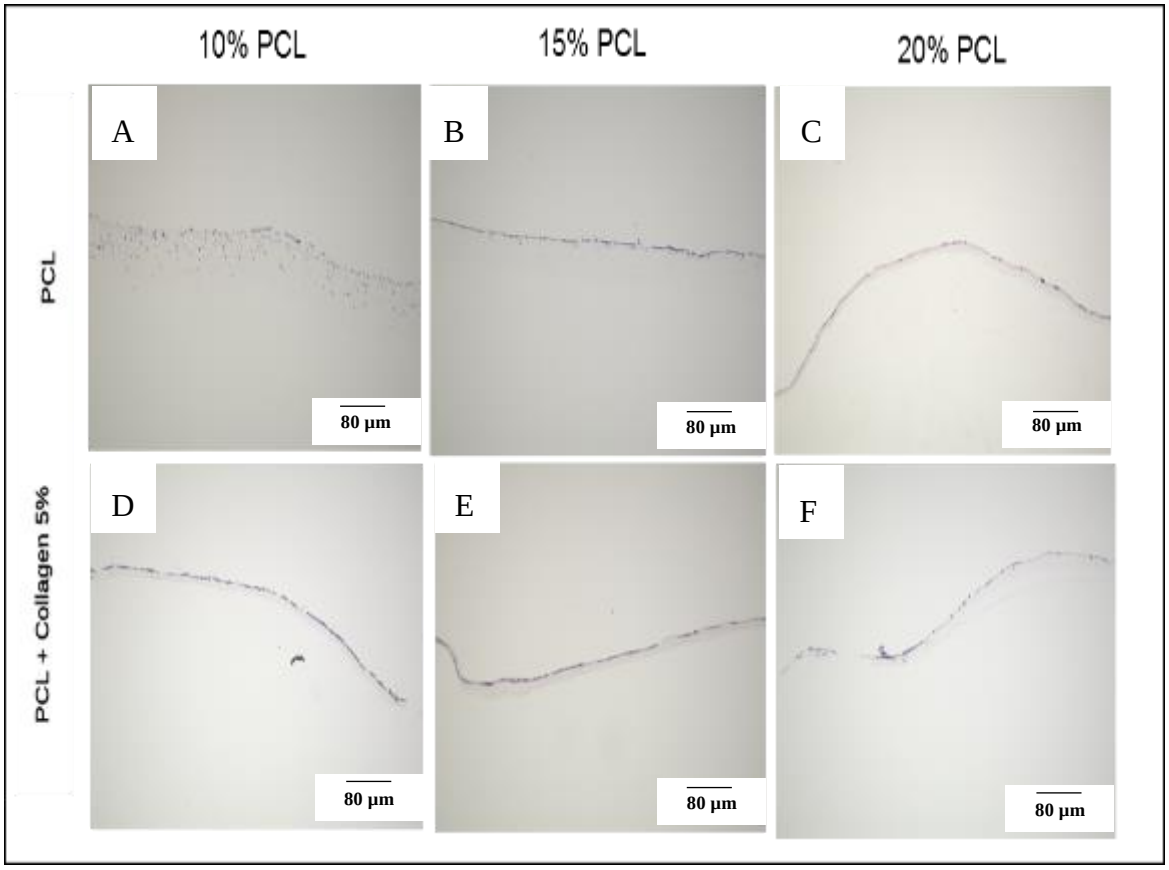

Figure 14. H&E Staining after scaffold cultivation in cell crowns *(10-fold magnification)*

Using immunohistochemically staining (Figure 15) confirmed that isolated and then seeded cells are CD31 positive. Platelet endothelial cell adhesion molecule (PECAM-1) also known as CD31 makes up a large portion of endothelial cell intercellular junctions and is primarily used to demonstrate the presence of endothelial cells. With this staining it is proven that these scaffolds were seeded with mostly hmvECs. Here, is once again to see that endothelial cells tend to create one single layer of cells. The pure PCL scaffolds revealed inferior results compared to multilayered scaffolds.

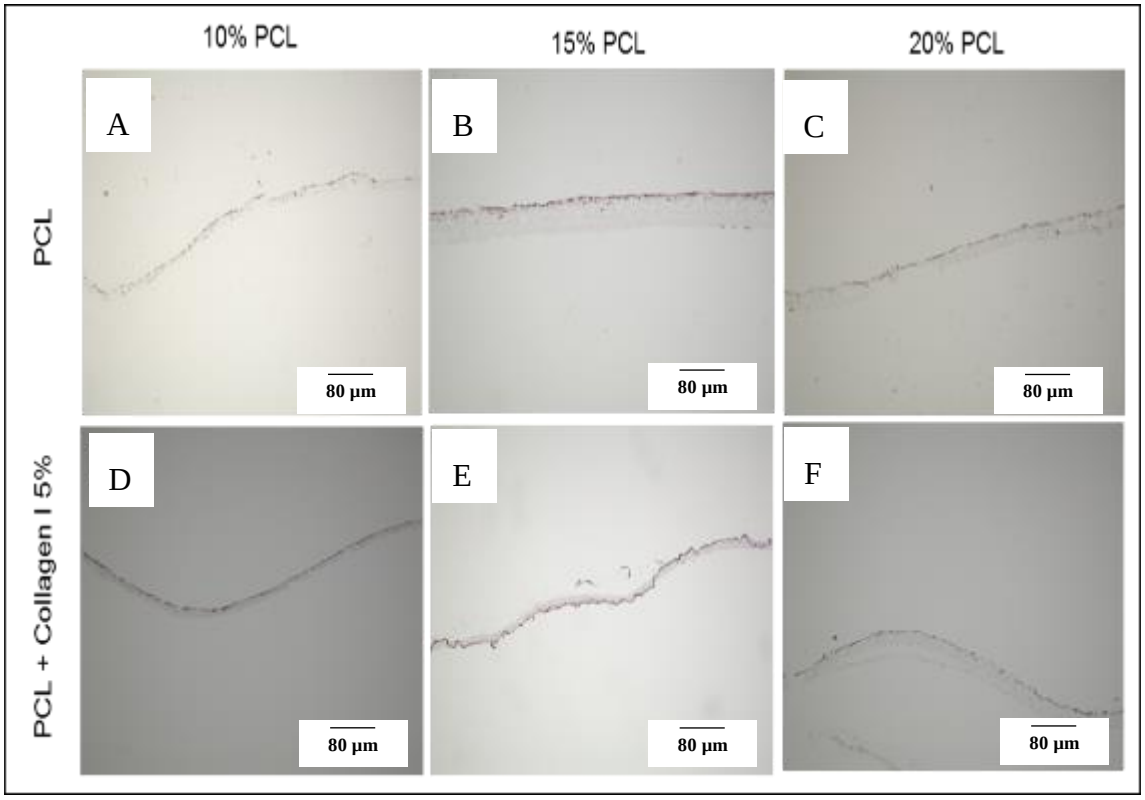

Figure 15. Immunohistochemistry with CD31. *(10-fold magnification)*

A quantitative MTT Assay was performed to investigate cell viability, as only the viable and metabolically active cells are able to reduce tetrazolium salt in blue formazan. Moreover, quantification via spectrophotometry is possible. No statistical significance (*p* = NS, Figure 16 B) between pure PCL scaffolds made of different PCL concentrations was found. However, when comparing pure PCL and multilayered PCL/collagen scaffolds, a statistical difference in viability ($p<0.05$) was detected. Most of the cells viable on all scaffolds after 7 day of cultivation which was also confirmed Live/Dead Staining (Figure 17).

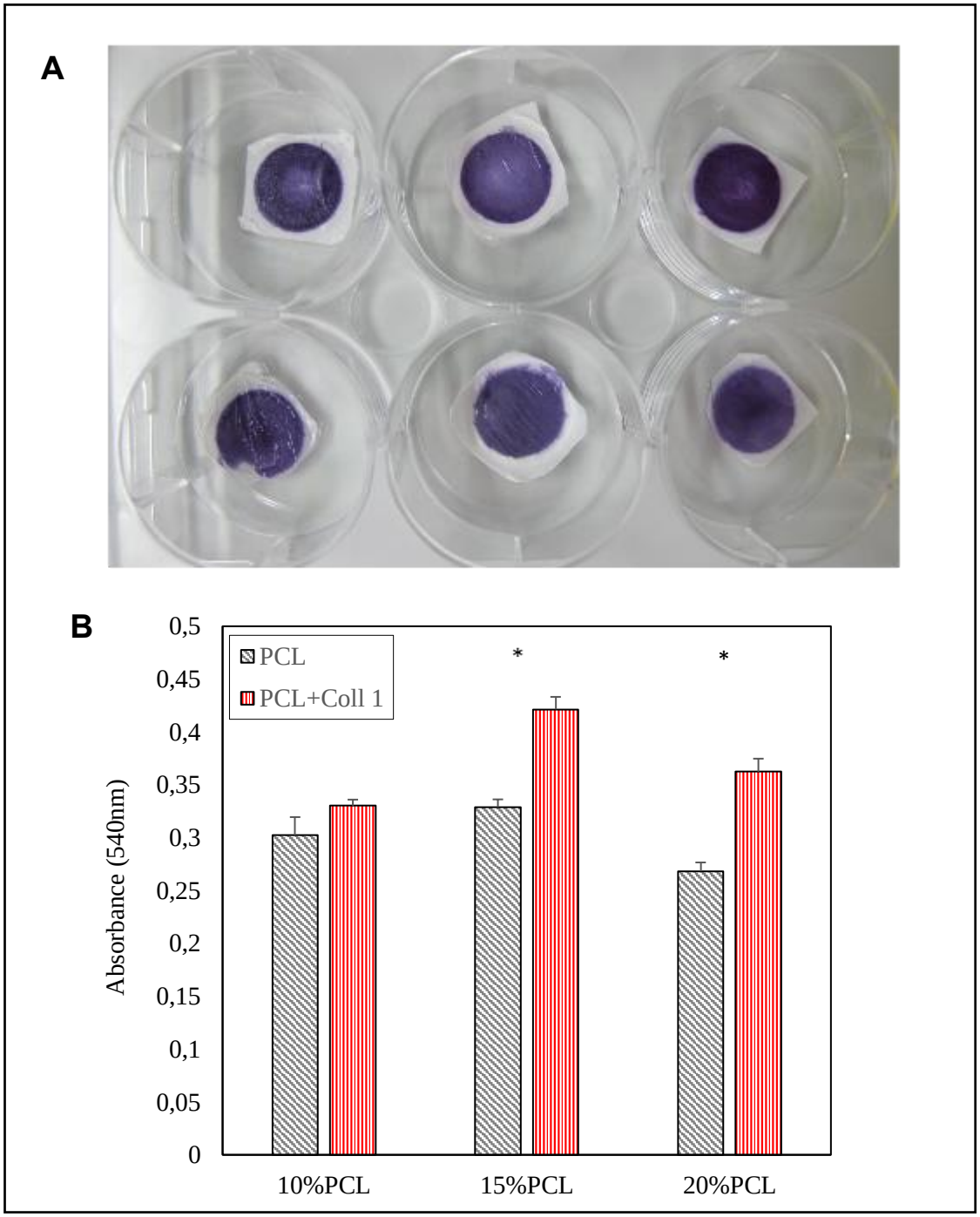

Figure 16. MTT Assay of scaffolds after static cultivation. *A – Qualitative Test shows purple color of formazan, proving viable cells on all types of scaffolds. B – Quantitative analysis on Tecan reader (* $p < 0.05$).*

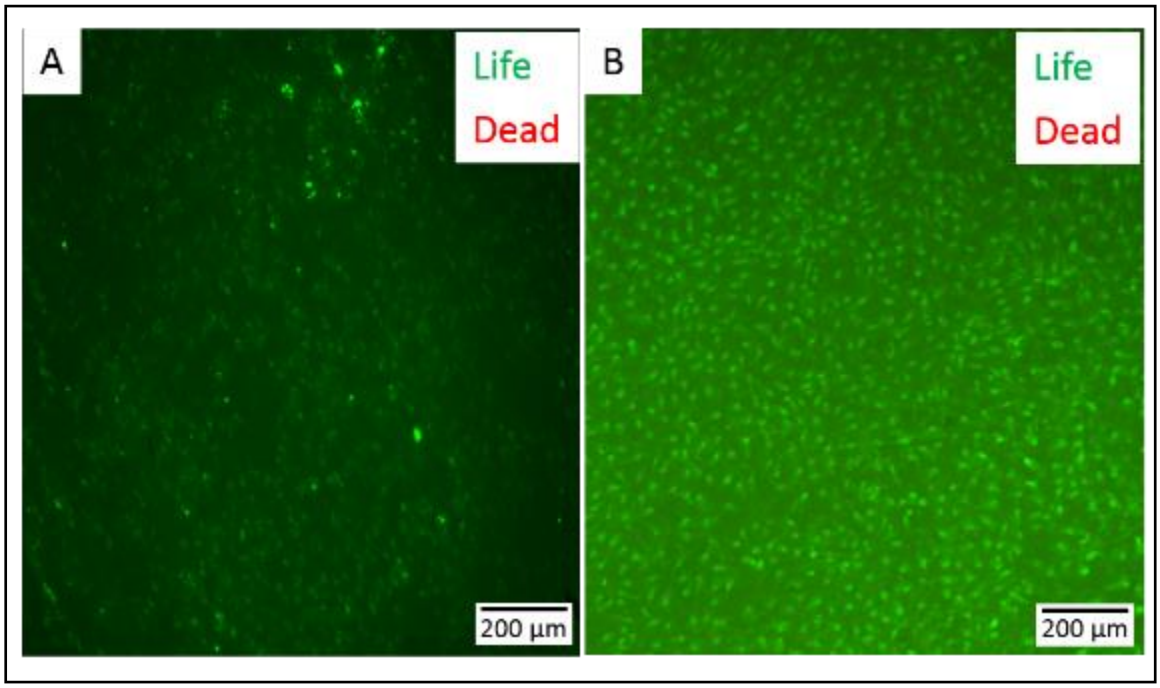

Figure 17. Live-Dead Staining. *hmvECs after static cultivation on PCL scaffolds (A) and multilayered PCL/collagen scaffolds (B). (Also used for publication in PLoS ONE (1))*

Further on acetylated-low density lipoprotein (Ac-LDL) was used to label hmvEC and to show activity of the scavenger pathway. (59) After 7 days cultivation, all hmvECs on both types of scaffolds demonstrated a high acLDL uptake (Figure 18A), and after

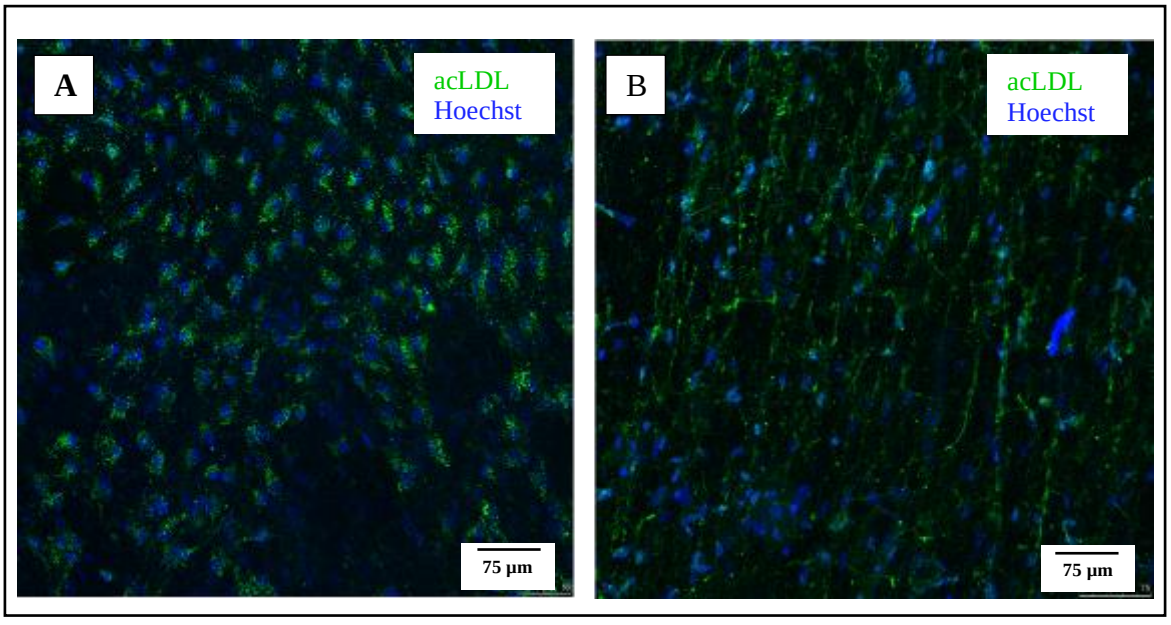

Figure 18 acLDL test. *(A) static culture in cell crowns, (B) dynamic culture in flow bioreactor. (Also used for publication in PLoS ONE (1))*

cultivation in bioreactor system it was detected that inner layer consists out of endothelial cells which have remained metabolically functional.

5.3. Cellular infiltration and phenotypic maintenance in the continuous flow bioreactor system

After static cultivation, it was decided to use multilayered PCL/collagen grafts because of better cell organization and higher cell viability on this scaffolds for dynamic culture experiments. In order to improve cellular infiltration and organization so that cells cover the full circumference of the grafts, the multilayered tubular scaffolds were filled with hmvECs and incubated in the pulsatile bioreactor system (Figure 10 - Figure 11).

After 14 days, H&E staining were performed. Thereby, a cell layer lining the whole circumference could be seen. Additionally, cells partially migrated into the scaffold, which was not to be detected in static cultures (Figure 19A). Phenotypic expression of endothelial markers, such as CD31+ and vWF was confirmed in the inner layer of our grafts also after cultivation in flow reactors (Figure 19B-C).

Expression of this antigens was also high in cells, which migrated in the scaffolds, but nevertheless continuous monolayer of cells is clear to be seen on the luminal side. In immunofluorescence with collagen type I marker, it is proved that grafts are multilayered, where collagen layer is clear to be seen on inner and outer side of the graft (Figure 19D).

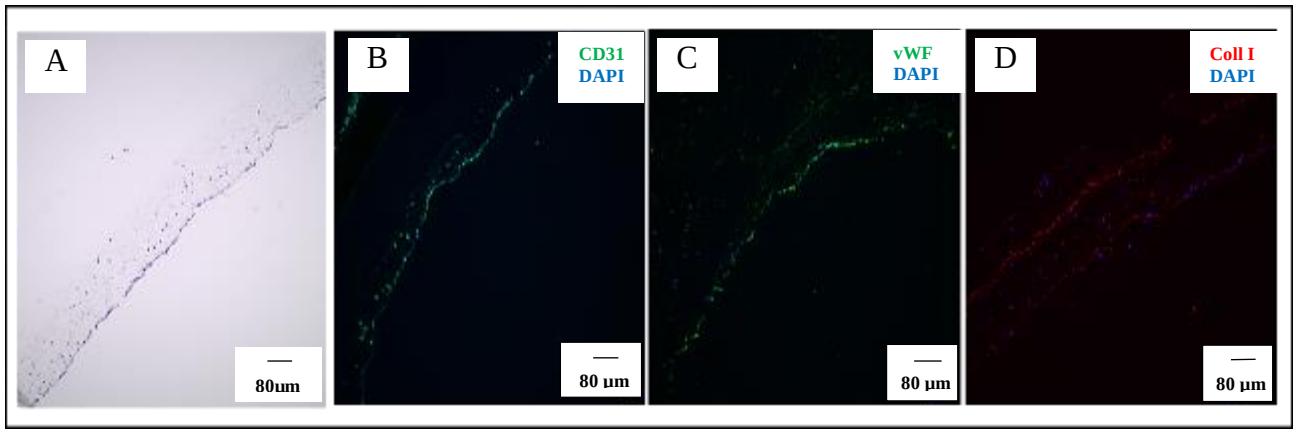

Figure 19. Electrospun vascular grafts after incubation in flow bioreactor system. *(A) - H&E Staining, (B) – CD31+, (C) – vWF, (D) – Collagen type I.*

In MTT Assay, cells covering the inner layer of the graft showed increased reduction of tetrazolium into blue formazan, so that a high viability rate of the endothelial cells covering the luminal side of the grafts is proved.

AcLDL uptake was also high in the endothelial cells after incubation in flow bioreactor systems (Figure 18B). In this test it is also possible to see that after incubation in dynamic bioreactor system the endothelial cells have started to organize in the flow direction compared to static cultures. All these results indicate that flow conditions have provided increased cellular infiltration and organization on the luminal side of the grafts while maintaining hmvECs phenotype and viability.

5.4. Bioactivity of antibiotics loaded scaffolds

The effect of the vancomycin/gentamicin loaded scaffolds was evaluated in using the zone of inhibition testing. After electrospinning with vancomycin and gentamicin (only in middle PCL layer), the multilayered scaffolds were placed on plates previously seeded with *Staphylococcus aureus and epidermidis*. The maximum mean diameter of the inhibition zone in the presence of *Staphylococcus aureus and epidermidis* was 14.5 ± 0.48 mm and 20.5 ± 0.5 mm on the first day (Figure 20A-B), respectively. Over the next 28 days the diameter of the inhibition zone increased and remained unchanged over the observed period (Figure 20C). The measurements were performed on every second day.

MTT Assay was also performed after seeding the hmvECs on these scaffolds which were enriched with antibiotics to test the cytotoxicity of such scaffolds. Only static cultures as described in 4.11. were performed.

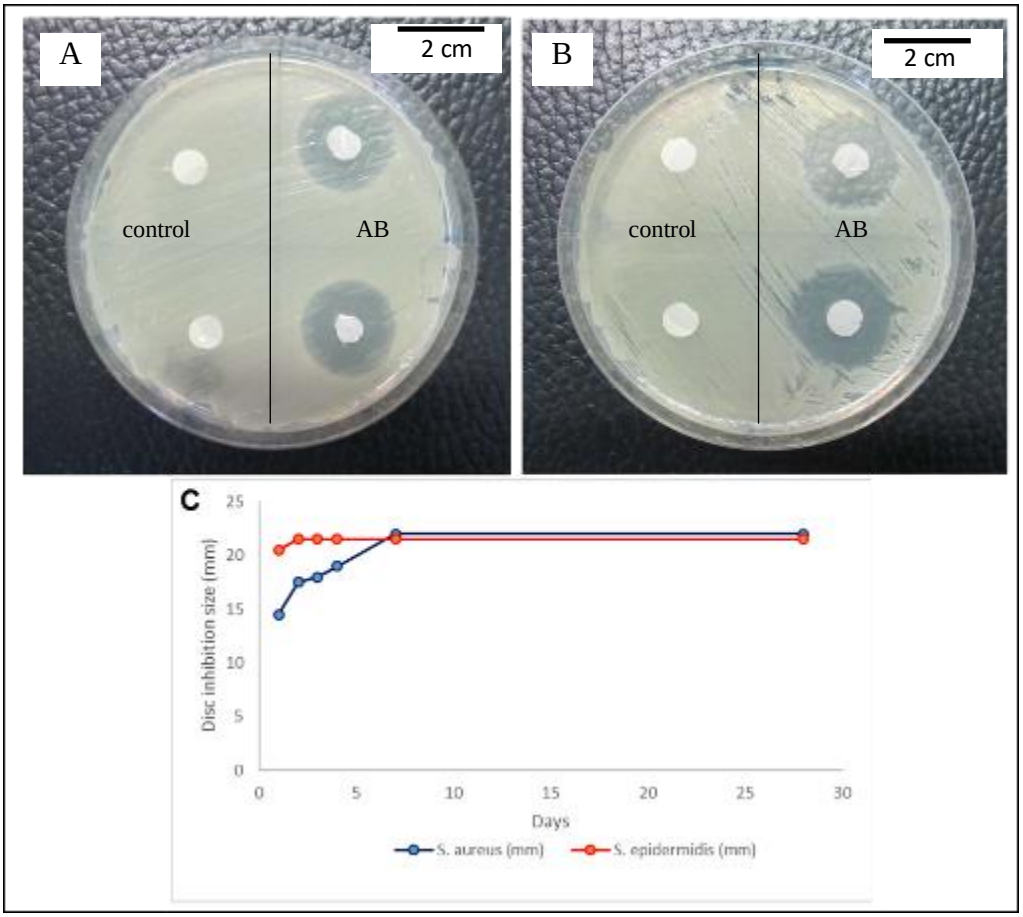

Figure 20. Antibacterial efficacy. *On the (A) is Staphylococcus aureus inhibition and on (B) Staphylococcus epidermidis. (C) shows the change in the size of inhibition zone for both pathogens over the period of 28 days of observation. (A and B - also used for publication in PLoS ONE (1))*

In the qualitative MTT assay, scaffolds loaded with vancomycin and gentamicin and seeded with hmvECs showed also high cell viability by changing the color of MTT reagent from yellow into violet (Formazan) after 2 hours of incubation. Moreover, the surface of seeded scaffolds was dyed violet, demonstrating viable cells proliferating on such scaffolds. In quantitative analysis, an even higher rate of tetrazolium reduction was show when compared to same multilayered scaffolds without antibacterial loading. This anyway interesting result, showed no statistical significance (Figure 21, p = NS). All this demonstrated that adding antibiotic loading into multilayered scaffolds with its local in

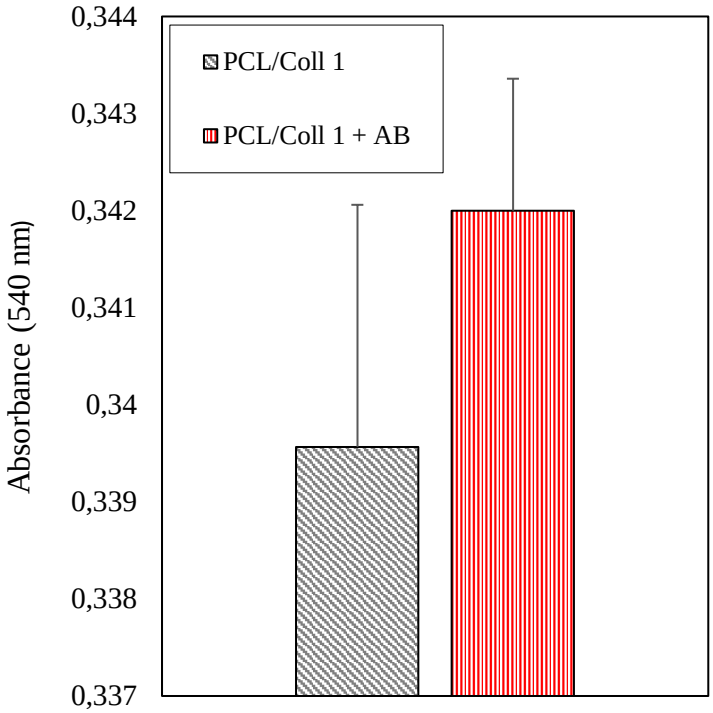

Figure 21. MTT Assay of scaffolds loaded with antibiotics. *(p = NS)*

situ effect may lead to reduction of infection rate without endangering the native cell proliferation. Further studies regarding this problematic are needed.

6. Discussion

The aim of this work, was to develop an artificial, small vascular graft, which can be used as vascular access for hemodialysis. The potential of such small vascular grafts in modern cardiovascular surgery, especially for all types of aorto-coronary bypass or any other peripheral arterial bypass surgery is obvious. In the study presented here, an electrospinning process was harnessed to manufacture tubular scaffolds with mechanical and biological properties appropriated for vascular grafts. In addition to the identification of suitable polymers, scaffolds were characterized regarding their morphology and mechanical properties. The biological evaluation of vascular grafts was performed by using human endothelial cells that were cultured under static and dynamic conditions. The culture in the bioreactor system facilitated the endothelial cell proliferation and coverage of luminal surface. Moreover, antibiotics were successfully incorporated into the graft. Thereby, the risk of an initial infection as one of the most important complications of hemodialysis after vascular graft implantation can be reduced.

The number of patients suffering end stage kidney disease is growing and vascular access remains a major medical problem for these patients. (60) An arteriovenous fistula represents the first choice for hemodialysis access. However, when these are not available, prosthetic grafts such as polytetrafluoroethylene (ePTFE) serve as alternative, although they are associated with increased morbidity and mortality (61). Moreover, synthetic grafts don't match the efficacy of autologous blood vessels, particularly when graft diameter is $\leq$ 6 mm. (62, 63) The field of TE offers alternatives to classical approaches with more or less success in the past decade. (37, 57) The aim of TE is to develop functional tissue in vitro. These tissues can either be implanted in patient to replace damaged organ or used as a test system for experiments in pharmacologic or medical devices industry. In both cases, tissues need to be comparable to native tissue and poses the same or similar morphology and functionality. Cells, scaffolds and growth-stimulating signals represent the key components of engineered tissues. Hereby, scaffolds provide structural support for cell attachment and tissue development. This identifying a suitable material for a certain application is the first obstacle in TE process. Nanofibrous scaffolds produced using the methods of electrospinning have advantages such as a good

resilience against mechanical stress. Furthermore, electrospun scaffolds presuppose orientation of cells by fiber orientation.

Beside of being a challenge itself, production of dialysis graft mimicking native vessel structure needs to answer further criteria and demands such as to be easily implanted, non-thrombogenic, biocompatible, resist aneurysmal dilatation and to be able to lower risk of onsite infection after implantation despite repeated needle trauma. Experiments with naturally derived materials such as collagen and elastin have been considered due to their biocompatibility characteristics. However, such scaffolds showed significant mechanical instability. On the other hand, synthetic polymers such as PLGA provide structural support. Nevertheless, biocompatibility is impaired compared to natural materials. Polyurethanes have also been used, but these materials are not degradable. (64) In this study, PCL was chosen because it is biodegradable, it is well-known for its elasticity, and it is already medically approved by Food and Drug Administration (FDA). Sequential electrospinning was performed, whereby the collagen type I and PCL flow ratio increased and decreased simultaneously, so that at the beginning and the end of the process only collagen type I and in the middle only PCL was deposited. As a result, the luminal and outer layer were made only of natural material ± collagen type I. Collagen type I was favored as the major component of a native vessel and due to its described biocompatible properties. PCL, a medically-approved elastic polymer, allowed to tailor graft strength in order to endure physiological hemodynamic conditions. (57) The earliest collagen-based scaffolds manufactured by electrospinning were produced by Huang et al. However, these scaffolds were composed of collagen combined with polyethylene-oxide (PEO) instead of the pure natural polymer. (65) A year later, Matthews et al. published the first work of successful electrospinning of pure collagen type I and II. (40) Most of the reports to date describe use of electro spun collagen scaffolds as wound dressing and vascular grafts. Moreover, it was shown that SMC and ECs prefer collagen over synthetic materials, but on the other side due to high intraluminal pressure it is likely that pure collagen scaffolds lead to mechanical failure. (66, 67) Combination of PCL and collagen electrospinning has already been tested, whereas most of this work is based on either coating the collagen layer on electrospun PCL, where the risk of delamination is higher, or mixing the both polymers in one solution and electrospinning them together on collector. Also, electrospinning of more natural proteins has been described when

Buttafoco with his group electrospun collagen together with elastin. However, mechanical test were not performed. (68) The production of multilayered vascular grafts was previously described by Xiumei Mo and his group. Therefore, different polymer solutions in separate syringe pumps were used. The polymers were placed opposite to each other to perform bidirectional electrospinning. (69) They showed combination of good mechanical properties and sufficient biocompatibility, whereas in this work only static cultivation was used.

Multilayered vascular scaffolds were produced using the coaxial electrospinning with regulated environment conditions. Electrospinning is effective and cost-efficient method which uses electrical force to draw charged threads of polymer solutions to produce micro- or nanofibers with suitable porosity enabling a good cell adhesion and growth. For this purpose, a custom-made device was made in the Chair for Tissue Engineering & Regenerative Medicine, University Würzburg. It provides the possibility of bidirectional gradient electrospinning of two different polymers from opposite spinnerets on rotating mandrel, and all this in a closed chamber with stabile temperature and humidity. Bidirectional electrospinning enables production of multilayered scaffold composed of two different polymers. Therefore, it is important to choose the suitable solvent and the polymer concertation which provide the best results. First test showed that the best solvent for PCL scaffolds is HMDI, and increasing concentrations from 10 to 25 % showed good electrospinning performance. Higher polymer concentrations were too dense to form and withhold a Taylor cone on spinneret during electrospinning process. On the other hand, lower concentrations led to prompt solutions squirting solvent drops in the collector direction not being able continuously to produce nanofibers. For these experiments, collagen was dissolved in TFE and the most suitable polymer concentration in this case was 5 %. With this concentration, it was possible to continuously spin collagen nanofibers on the collector without having solvent drops on the scaffold. Also, the Taylor cone was the most persistent and continuous when this concentration was used.

SEM observations confirmed that both polymers PCL and collagen during electrospinning process formed continuous fibers. Electrospinning was performed in that manner that collagen and PCL flow ratio increased and decreased simultaneously as shown in Table 9, so that at the beginning and the end of the process only collagen was

flowing and in the middle only PCL. As a result, the luminal and outer layer were made only of natural material – collagen (Figure 19D). By adding transitional layers in between, when both polymers were electrospun, the risk of delamination was decreased. This was supported during the experiments in dynamic bioreactor, where grafts were exposed to mechanical stress. Collagen type I, as the major component of a native vessel and because of its known biocompatibility was combined with polycaprolactone, a medically approved elastic polymer. This was done with the idea of improving graft strength needed to endure physiological hemodynamic conditions.

Since relative humidity also plays a key role in electrospinning (70), the whole process was performed in the closed chamber with the stabile climate. Analyzing SEM images, it was found that the most suitable porous structure is produced, when the relative humidity stays below 30 %. The relative humidity during vascular graft production was controlled to be 27 ± 2 % and temperature 2 °C. Through the SEM observations, it was confirmed that both pure PCL and multilayered PCL/collagen type I scaffolds were formed of continuous nanofibers under all solution concentrations and flows used in the study.

Fibers in the multilayered vascular grafts revealed a higher diameter without changes in pore sizes, in contrast to PCL vascular grafts, thereby representing a suitable substrate for cell attachment and growth of hmvECs. Furthermore, the addition of a collagen layer onto a PCL structure in the multilayered grafts significantly increased hydrophilicity, which had a positive effect on cell adhesion, proliferation and migration. Changing the temperature and humidity conditions in the electrospinning chamber resulted in changes of vascular graft microstructure. Thicker fibers with smaller pores were produced on the luminal side and bigger pores on the outer layer allowing proliferation and migration in the vascular graft.

The ANSI guidelines (Association for the Advancement of Medical Instrumentation American National Standards Institute. Cardiovascular implants—Tubular vascular prostheses. Arlington, VA: AAMI; 2004.) recommend to measure both longitudinal and circumferential force of the vessels, burst pressure, and suture retention strength. PCL vascular grafts showed superior tensile strength compared to multilayered grafts and higher elongation properties, which should prevent graft inflation when pressure is

increased. The results for the PCL scaffolds were comparable to results reported by other authors. (71) Multilayered vascular grafts showed tensile strength inferior to PCL, with lower elongation properties. Similar results were reported from groups, who blended these two polymers and showed higher elongation and tensile strength in PCL scaffolds compared to ones blended with collagen type I. (72) Young's Moduli were calculated for the multilayered grafts by assuming a material thickness of 10 μm. PCL scaffolds showed a higher elastic modulus compared to multilayered vascular grafts as shown in Figure 13A. Similar results were demonstrated by Xiumei Mo and his group, when comparing pure PCL and multilayered scaffolds with an additional outer layer composed of chitosan. They also showed different mechanical properties of grafts in dry and wet state, demonstrating results favoring multilayered scaffolds in wet state. (69) All mechanical tests in this study were performed in dry state.

Further testing of burst pressure and suture retention strength are important to ensure that the graft can withstand the surgical manipulation during implantation and physiological pressure after implantation. The average pressure in the arterial circulation is 100 mmHg, and is higher in leg arteries while standing. Due to the contribution of hydrostatic pressure, pressure values can reach up to 250 mmHg. (73) In our experiments, despite different tensile strength properties, we have shown no significant difference in pressures, which led to graft failure between PCL and multilayered grafts. Mrowczynski et al. showed good surgical friendliness and in vivo characteristics of pure PCL grafts. When implanted in rat's infrarenal artery and porcine carotid artery no graft failure due to physiological pressure was observed. (74) The mechanical stiffness and burst pressure needed for arterial implantation is not defined but studies have shown that burst pressures of 600±700 mmHg can be implanted without significant dilatation in porcine models. (75) In this study, multilayered vascular graft containing 15 % PCL and collagen type I sustained max. 664 mmHg (Figure 13D). This multilayered scaffold was used further on, for in vitro dynamic seeding with hmvECs. When considering suture retention strength, multilayered grafts showed a lower force required to pull the suture through the graft compared to pure PCL grafts, which were comparable to the values of native vessels ranging between 0.8 N to 2.5 N reported in other studies. (76) In further experiments, increasing the thickness of the middle PCL layer, which might lead to even better suture retention strength in multilayered vascular grafts will be considered.

Surface wettability of biomaterials is known to affect cell adhesion, proliferation and migration. In this work, it was shown how addition of collagen layer to PCL in multilayered scaffolds increased significantly hydrophilicity of scaffold. This resulted in a positive effect on cell adhesion and proliferation as shown in MTT tests, where violet color of formazan could be detected on multilayered scaffolds to higher extent as compared to pure PCL scaffolds.

Beside the need of excellent mechanical properties, the vascular graft needs to be biocompatible to accommodate vascular cells while maintaining structural integrity. In this study, the cell crowns were first used as static systems to test adherence tendency of hmvECs towards different electrospun scaffolds. Cultivation in cell crowns has a few advantages, first the cells tend to stay on the scaffolds and not fall on the side together with medium. Cell medium stays inside the cell crown and can easily be changed without the risk of damaging the upper surface where cells proliferate or aspirating the cells together with medium. One advantage of such static cultivation system is possibility of cultivation different cell lines on different sides of scaffold (upper and lower) and possibility of using different cell mediums if needed (the inner and outer chamber of a cell crown are isolated). In this experiment, only one cell line (hmvECs) were used. Nevertheless, in further investigation a combined cultivation of hmvECs and SMCs is obvious. On all scaffolds, both pure PCL and multilayered, hmvECs adhesion and proliferation is demonstrated after 7 days. Quantitative analysis of pure PCL scaffolds and PCL/collagen scaffolds showed statistically higher viability rate in multilayered scaffolds probably due to higher hydrophilicity and slightly bigger nanofiber size, presenting possibly bigger surface for cell adhesion. Due to this, only these multilayered scaffolds were used in dynamic bioreactors to test the capability of such scaffolds to maintain cell adherence.

The use of dynamic tissue reactors in vascular TE has, compared to traditional cell culture techniques, advantage of adding additional aspects important to improve the vascular grafts properties in vitro. Mechanical stimulation by flow and sheer stress promote functional, cell seeded graft formation. In this study, a bioreactor was custom made for vascular graft TE. The tubular scaffold itself is clamped between two tubules and tied firmly. The tubules were connected with tubes, and this over a rotor pump with a bottle

filled with culture medium. The system in whole can be seen in Figure 22. Thereby, the cell medium was continuously pumped through the inner lumen of the graft scaffold. One bigger tube was pulled over the whole construct so that one additional outer chamber is created. The outer tube as well as the inner tubes on the side are filled with the medium so that cell culture medium flowed also on the outer side of the graft (Figure 22A). With this construct, it can also be achieved that different cell mediums circulate separately through the inner graft lumen and outside the graft if needed. In this study, the medium flow and sheer stress represent the most influential factors to imitate a vascular flow environment.

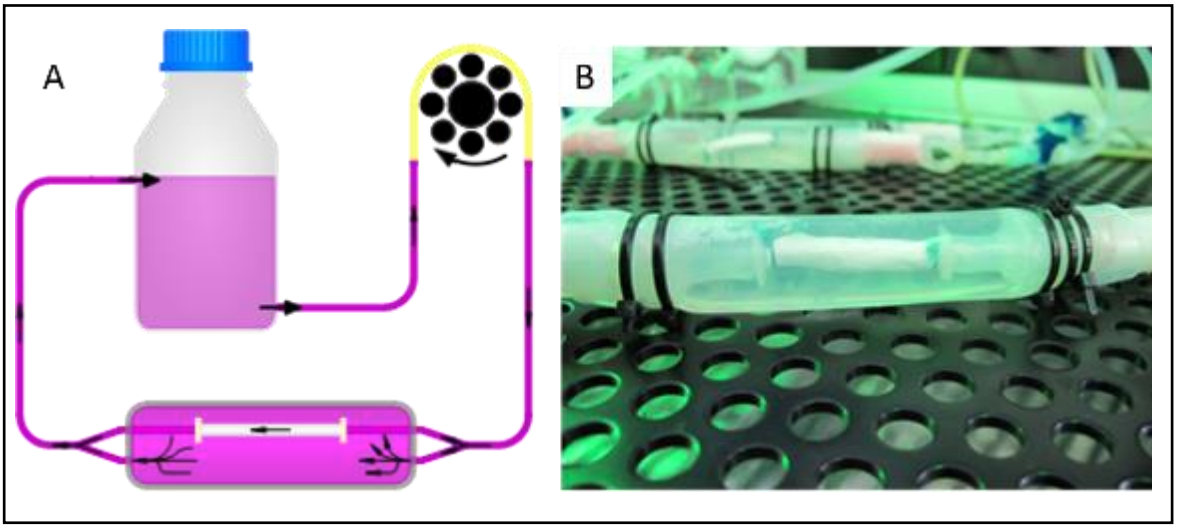

Figure 22. Bioreactor construction. *Dynamic culture of tubular vascular grafts was performed in a (A) perfusion bioreactor system inside a closed chamber with controlled environment conditions The TEVG is clamped between two tubes and tied firmly. Cell culture medium flow inside the graft due to tubes and pump system, but also the outer chamber of bioreactor was filled with cellular medium (B). (A - Also used for publication in PLoS ONE (1))*

H&E stain of both static (Figure 14) and dynamic cultures (Figure 19A) showed the tendency of endothelial cells to organize in one single layer. After cultivation of cells in dynamic flow bioreactor, it was observed that cells tend to organize circumferentially, keeping single layer organization. Additionally, in MTT staining it is proved that viable cells have adhered and grown mainly on the luminal side of graft during incubation under dynamic conditions. Rapid endothelial coverage of the surface is mandatory as this surface is in direct contact with blood flow and is also necessary to offer anti-thrombosis

property to acquire long-term patency as endothelial integrity represents important part of Virchow's triad. (77) In this model, endothelial cells tend to completely cover the scaffolds within one week of static cultivation, but also after 10 days cultivation in dynamic bioreactor. Hereby, it is important to stress that the incubation time in the dynamic bioreactor was 10 days compared to 7 days static cell culture. Although a longer culture duration was performed in contrast to static culture, the required dynamic culture period was shorter compared to durations reported by other groups, who performed 14 days incubation preceded with 3 days static cell culture. (78, 79) This way with collagen as inner layer superior seeding properties are shown, and dynamic cultivation can be started without prior static cell culture.

Further on, phenotypical and functional assays on scaffolds seeded with endothelial cells were performed. After incubation in dynamic flow bioreactor it was possible to detect vWF and $CD31^+$ expression, as one of characteristics to confirm endothelial identity. Also in this immunohistological findings, tendency of endothelial cells to organize in one single layer and to cover the luminal side of graft can be seen. This way positive effect of MACS sorting was demonstrated, favoring majorly endothelial cells and reducing the risk that the scaffold may be overpopulated with other cell types, fibroblasts for example. This also confirmed cytocompatibility of PCL/collagen grafts. To some extent hmvECs can also be seen inside the scaffold after cultivation. This might be due to higher sheer stress in flow bioreactor at the beginning of the cultivation before the single layer is formed which pushes the cells deeper in the scaffold or due to randomly bigger pores in the scaffold. In future experiments this can be reduced either by keeping the medium flow at the begin of cultivation at lower level, and increasing it after some time or by further manipulating the pore size in scaffold also by means of changing environment conditions.

Further on, uptake of acetylated LDL through scavenger receptor mediated endocytosis was tested and confirmed. This proved that endothelial cells after seeding on electrospun scaffolds remained functional and were able for active transport of molecules. (59, 80) Moreover, using this for fluorescent staining of living cells after cultivation in dynamic flow bioreactor it was noticed that endothelial cells were organized and aligned in one direction (Figure 18B). A continuous endothelial layer as such represents an important atheroprotective aspect. (81)

One more important aspect of this study is vascular graft infection. The incidence of graft infection is reported between 1 % and 6 % (82, 83) , whereas mortality varies between 25 to 75 % and plays one of the most important reason of deaths of dialysis patients. (84, 85) Hence, it is investigated if such electorspun vascular grafts can be combined with antibacterial agents to reduce the risk of vascular graft infection. Various tests and studies were performed to reduce implant related infections, based either on repelling or directly killing pathogenic agents. Biofilms play most important role in this task, are especially hard to remove and show significant resistance to all type of biocides. The best option of preventing vascular infection is prevention of biofilm formation on graft surfaces by reducing the adhesion of microorganisms. This is possible either by repelling or direct killing pathogens. Repelling can be achieved by charging the polymers or by hydrophobic modifications, such as coatings with PEG. Killing of pathogens can result of either releasing a biocide directly from matrix or by attaching antimicrobial polymers to surfaces. Silver ions were successfully coated with polymeric materials to cover the surface of vascular grafts prior to implantation. (86) Although colonies of *Staphylococcus aureus* were successfully inhibited without signs of cytotoxicity, the concept of covering the surface of vascular grafts with silver ions might compromise possibility of seeding smooth muscle cells on and inside these grafts in further studies. (87) There are a few techniques describing how to attach polymers to surfaces. These include grafting techniques, plasma polymerization and layer by layer depositions. (88-90) These techniques showed to be useful but not wide-spread in the industry because of their high price. All these techniques result in surfaces that kill microbial cells when they come in contact with them, without releasing a biocide. Other groups tested different antibiotics to facilitate local antimicrobial effects in cases of diverse surgical site infections. (91-93) In this study, vancomycin and gentamicin were added in PCL solution as it formed a middle hydrophobic layer, in which antibiotics are expected to endure longer. Thereby, cell seeding on both sides of the graft also remains as option in perspective. It is known that *Staphylococcus epidermidis* and *Staphylococcus aureus* are most common bacteria in surgical graft infections so in this study the focus was on these pathogens. (94) After implantation, a relationship develops between bacterial cells and hosts own cells. (95) Survival competition between host's own cells and bacterial cells is crucial, and once when bacterial cells overtake the host and directly interact with the implant a biofilm is

formed in which bacterial cells are better protected against antimicrobial agents and immune system. (96, 97) To prevent this, and to increase local antimicrobial activity and allow a low cytotoxicity, vascular grafts should provide incompatible environment for bacteria and reduce the risk of infection after graft implantation. Grafts incorporated with vancomycin and gentamicin significantly inhibited *Staphylococcus aureus* and *Staphylococcus epidermidis* growth in bacterial cultures, and these remained inhibited for period longer than 28 days. Furthermore, MTT assays showed that such grafts incorporated with antibiotics had no negative effect on cell viability. This implicated that such grafts beside bacterial inhibition are not expected to have negative effect on host cell adhesion and proliferation. This preliminary investigation showed that this concept has potential, whereas further tests are needed particularly to test antibiotic release rate from such grafts in vitro and its efficacy in vivo after graft implantation.

7. Conclusion

In this work, it is shown that multilayered PCL/collagen type I electrospun scaffolds represent a suitable scaffold for small vascular grafts. The combination of synthetic and natural polymers can be seeded with hmvECs. This was proven during incubation in static system in cell crown as well as in dynamic continuous flow bioreactor. An endothelial lining can be achieved in chosen vascular scaffolds, and high purity of isolated cells has been shown. It has also been proven that hmvECs after isolation, cultivation and proliferation on such scaffolds remain functional by showing still active scavenger pathway, typical for this type of cells. Also, endothelial lining of the inner layer of small vascular graft provides important antithrombogenic property. The facilitated a high degree of patency and structural integrity during the whole period of in vitro incubation, and no structural changes, degradation or malformations have been shown during the incubation periods in flow bioreactor systems. Benefits of antibacterial loading of these TEVG are clear. Hereby, a high local antimicrobial activity of scaffolds after loading with antibiotics was demonstrated. As such, they represent an important advantage, whereas high biocompatibility remained. In summary, this study indicates that electrospun scaffolds might have potential for clinical application as alternative to traditional prosthetic graft materials in always increasing problem of providing vascular access for patients on hemodialysis.

8. Outlook

It is shown that functional and viable small diameter vascular grafts, which potentially can be used as hemodialysis access can be produced using the methods of TE. Electrospinning takes place in the closed chamber, so that the environment conditions are to some extent stable during the whole process. This way there is no significant variation in fiber and pore size in our scaffolds. Further development of this setting in sine actively influencing and adjusting the environment during electrospinning process is needed. For example, known and previously stated temperature and humidity play also important role in electrospinning and both have influence on fiber morphology. Thus, humidifier has already been added to the setting. Now it is possible to actively change the humidity in electrospinning chamber. Further experiments are needed to determine optimal conditions for the best scaffold morphology and further optimization of mechanical properties.

In future experiments, further tests should be undertaken to try to seed also smooth muscle cells (SMCs) on outer sides of the scaffolds. SMCs play an important role in maturity of blood vessels and contribute to contractility/tone and accelerate tissue maturation that provides mechanical stability for long-term patency. Cell crown construct for static cultures can enable seeding of SMCs. Therefore, the opposite side of scaffolds is accessible by simply turning the crown upside down. It also offers the possibility of using two different cell mediums on the upper and lower side of scaffold if needed. This way, on one side of the scaffold hmvECs can be seeded and on the other side SMCs. Furthermore, the bioreactor system described in this work with its isolated outer chamber offers also the possibility for cell seeding on the outer side of vascular graft and perfusion of this chamber side with different cell medium when separate tubes connected. According to this approach the complete biological vessel with its all major histological components might be produced. That way, beside its clinical potential it could also be used as a vascular test system for evaluation of drug efficacy in organ bath system for example.

For authorization of such small vascular graft in human medicine, animal studies are needed. The experiments on large animals are needed to test grafts morphological stability and functionality in vivo. Experiments on small animals may be the first step to test

biocompatibility according to ISO 10993-6 (local effects). However, only as graft for big arteries as rat aorta for example. Thereby, mechanical integrity of graft and tendency to blood leakage and aneurysmal changes might be controlled.

Finally, a preparation for good manufacturing practices (GMP) when producing small vascular grafts is needed. In this case, all culture mediums, substances and devices used in this experiment need to be authorized.

In the bottom line the search for the “holy grail” of small diameter vascular grafts remains, and this work present the complexity of such task. The ideal small vascular graft has to be affordable and comparable to native vessels regarding mechanical properties and biocompatibility. Also, decreasing the risk of local infection of such graft plays without doubt important role.

9. References

1. Radakovic D, Reboredo J, Helm M, Weigel T, Schurlein S, Kupczyk E, et al. A multilayered electrospun graft as vascular access for hemodialysis. PLoS One. 2017;12(10):e0185916.

2. Konner K. History of vascular access for haemodialysis. Nephrol Dial Transplant. 2005;20(12):2629-35.

3. Weinberg CB, Bell E. A blood vessel model constructed from collagen and cultured vascular cells. Science. 1986;231(4736):397-400.

4. Shin'oka T, Imai Y, Ikada Y. Transplantation of a tissue-engineered pulmonary artery. N Engl J Med. 2001;344(7):532-3.

5. Shin'oka T, Matsumura G, Hibino N, Naito Y, Watanabe M, Konuma T, et al. Midterm clinical result of tissue-engineered vascular autografts seeded with autologous bone marrow cells. J Thorac Cardiovasc Surg. 2005;129(6):1330-8.

6. Stevens PE, Levin A, Kidney Disease: Improving Global Outcomes Chronic Kidney Disease Guideline Development Work Group M. Evaluation and management of chronic kidney disease: synopsis of the kidney disease: improving global outcomes 2012 clinical practice guideline. Annals of internal medicine. 2013;158(11):825-30.

7. Foley RN, Chen SC, Collins AJ. Hemodialysis access at initiation in the United States, 2005 to 2007: still "catheter first". Hemodial Int. 2009;13(4):533-42.

8. Vascular Access Work G. Clinical practice guidelines for vascular access. Am J Kidney Dis. 2006;48 Suppl 1:S248-73.

9. Stolic R. Most important chronic complications of arteriovenous fistulas for hemodialysis. Medical principles and practice : international journal of the Kuwait University, Health Science Centre. 2013;22(3):220-8.

10. Hehrlein FW, Schlepper M, Loskot F, Scheld HH, Walter P, Mulch J. The use of expanded polytetrafluoroethylene (PTFE) grafts for myocardial revascularization. J Cardiovasc Surg (Torino). 1984;25(6):549-53.

11. Zilla P, Bezuidenhout D, Human P. Prosthetic vascular grafts: wrong models, wrong questions and no healing. Biomaterials. 2007;28(34):5009-27.

12. Brewster DC. Current controversies in the management of aortoiliac occlusive disease. Journal of vascular surgery. 1997;25(2):365-79.

13. Bos GW, Poot AA, Beugeling T, van Aken WG, Feijen J. Small-diameter vascular graft prostheses: current status. Arch Physiol Biochem. 1998;106(2):100-15.

14. Thomas LV, Lekshmi V, Nair PD. Tissue engineered vascular grafts — Preclinical aspects. International Journal of Cardiology.167(4):1091-100.

15. Biuckians A, Scott EC, Meier GH, Panneton JM, Glickman MH. The natural history of autologous fistulas as first-time dialysis access in the KDOQI era. Journal of vascular surgery. 2008;47(2):415-21; discussion 20-1.

16. Conte MS. The ideal small arterial substitute: a search for the Holy Grail? FASEB J. 1998;12(1):43-5.

17. Darouiche RO. Treatment of infections associated with surgical implants. N Engl J Med. 2004;350(14):1422-9.

18. Evans LV. Biofilms: Recent Advances in their Study and Control: Taylor & Francis; 2000.

19. Richards JJ, Melander C. Controlling Bacterial Biofilms. ChemBioChem. 2009;10(14):2287-94.

20. Stewart PS, Franklin MJ. Physiological heterogeneity in biofilms. Nat Rev Microbiol. 2008;6(3):199-210.

21. Kaplan JB, Izano EA, Gopal P, Karwacki MT, Kim S, Bose JL, et al. Low levels of β-lactam antibiotics induce extracellular DNA release and biofilm formation in Staphylococcus aureus. MBio. 2012;3(4):e00198-12.

22. Mienaltowski MJ, Birk DE. Structure, physiology, and biochemistry of collagens. Advances in experimental medicine and biology. 2014;802:5-29.

23. Molenaar JC. [From the library of the Netherlands Journal of Medicine. Rudolf Virchow: Die Cellularpathologie in ihrer Begrundung auf physiologische und pathologische Gewebelehre; 1858]. Ned Tijdschr Geneeskd. 2003;147(45):2236-44.

24. Loeb L. Über die Entstehung von Bindegewebe, Leucocyten und roten Blutkörperchen aus Epithel; und über eine Methode, isolierte Gewebsteile zu züchten. Chicago: Stern; 1897. 56 p. p.

25. Amit M, Carpenter MK, Inokuma MS, Chiu CP, Harris CP, Waknitz MA, et al. Clonally derived human embryonic stem cell lines maintain pluripotency and proliferative potential for prolonged periods of culture. Dev Biol. 2000;227(2):271-8.

26. Chan BP, Leong KW. Scaffolding in tissue engineering: general approaches and tissue-specific considerations. Eur Spine J. 2008;17 Suppl 4:467-79.

27. Kai D, Jin G, Prabhakaran MP, Ramakrishna S. Electrospun synthetic and natural nanofibers for regenerative medicine and stem cells. Biotechnol J. 2013;8(1):59-72.

28. Vasita R, Katti DS. Nanofibers and their applications in tissue engineering. International Journal of Nanomedicine. 2006;1(1):15-30.

29. Zeugolis DI, Khew ST, Yew ES, Ekaputra AK, Tong YW, Yung LY, et al. Electro-spinning of pure collagen nano-fibres - just an expensive way to make gelatin? Biomaterials. 2008;29(15):2293-305.

30. Zhang X, Reagan MR, Kaplan DL. Electrospun silk biomaterial scaffolds for regenerative medicine. Adv Drug Deliv Rev. 2009;61(12):988-1006.

31. Kucinska-Lipka J, Gubanska I, Janik H, Sienkiewicz M. Fabrication of polyurethane and polyurethane based composite fibres by the electrospinning technique for soft tissue engineering of cardiovascular system. Mater Sci Eng C Mater Biol Appl. 2015;46:166-76.

32. Hansmann J, Groeber F, Kahlig A, Kleinhans C, Walles H. Bioreactors in tissue engineering - principles, applications and commercial constraints. Biotechnol J. 2013;8(3):298-307.

33. Cleary MA, Geiger E, Grady C, Best C, Naito Y, Breuer C. Vascular tissue engineering: the next generation. Trends Mol Med. 2012;18(7):394-404.

34. Manduz S, Katrancioglu N, Ozker E, Dogan K. Early thrombosis in bovine mesenteric vein grafts after infrainguinal reconstruction. Int J Angiol. 2008;17(1):37-9.

35. Das N, Bratby MJ, Shrivastava V, Cornall AJ, Darby CR, Boardman P, et al. Results of a seven-year, single-centre experience of the long-term outcomes of bovine ureter grafts used as novel conduits for haemodialysis fistulas. Cardiovasc Intervent Radiol. 2011;34(5):958-63.

36. Kennealey PT, Elias N, Hertl M, Ko DS, Saidi RF, Markmann JF, et al. A prospective, randomized comparison of bovine carotid artery and expanded polytetrafluoroethylene for permanent hemodialysis vascular access. Journal of vascular surgery. 2011;53(6):1640-8.

37. McAllister TN, Maruszewski M, Garrido SA, Wystrychowski W, Dusserre N, Marini A, et al. Effectiveness of haemodialysis access with an autologous tissue-engineered vascular graft: a multicentre cohort study. Lancet. 2009;373(9673):1440-6.

38. Cooley JF. Apparatus for electrically dispersing fluids. Google Patents; 1902.

39. Doshi J, Reneker DH. Selected papers from the special technical session "Electrostatics in Polymer Processing and Charge Monitoring", 1993 IEEE Industry Applications Society MeetingElectrospinning process and applications of electrospun fibers. Journal of Electrostatics. 1995;35(2):151-60.

40. Matthews JA, Wnek GE, Simpson DG, Bowlin GL. Electrospinning of collagen nanofibers. Biomacromolecules. 2002;3(2):232-8.

41. Li WJ, Laurencin CT, Caterson EJ, Tuan RS, Ko FK. Electrospun nanofibrous structure: a novel scaffold for tissue engineering. J Biomed Mater Res. 2002;60(4):613-21.

42. Sun D, Chang C, Li S, Lin L. Near-field electrospinning. Nano Lett. 2006;6(4):839-42.

43. Malakhov SN, Khomenko AY, Belousov SI, Prazdnichnyi AM, Chvalun SN, Shepelev AD, et al. Method of manufacturing nonwovens by electrospinning from polymer melts. Fibre Chemistry. 2009;41(6):355-9.

44. Muerza-Cascante ML, Haylock D, Hutmacher DW, Dalton PD. Melt electrospinning and its technologization in tissue engineering. Tissue engineering Part B, Reviews. 2015;21(2):187-202.

45. Demir MM, Yilgor I, Yilgor E, Erman B. Electrospinning of polyurethane fibers. Polymer. 2002;43(11):3303-9.

46. McKee MG, Wilkes GL, Colby RH, Long TE. Correlations of Solution Rheology with Electrospun Fiber Formation of Linear and Branched Polyesters. Macromolecules. 2004;37(5):1760-7.

47. Zeng J, Haoqing H, Schaper A, Wendorff JH, Greiner A. Poly-L-lactide nanofibers by electrospinning–influence of solution viscosity and electrical conductivity on fiber diameter and fiber morphology. e-Polymers. 2003;3(1):102-10.

48. Zong X, Kim K, Fang D, Ran S, Hsiao BS, Chu B. Structure and process relationship of electrospun bioabsorbable nanofiber membranes. Polymer. 2002;43(16):4403-12.

49. Lee JS, Choi KH, Ghim HD, Kim SS, Chun DH, Kim HY, et al. Role of molecular weight of atactic poly(vinyl alcohol) (PVA) in the structure and properties of PVA nanofabric prepared by electrospinning. Journal of Applied Polymer Science. 2004;93(4):1638-46.

50. Buchko CJ, Chen LC, Shen Y, Martin DC. Processing and microstructural characterization of porous biocompatible protein polymer thin films. Polymer. 1999;40(26):7397-407.

51. Casper CL, Stephens JS, Tassi NG, Chase DB, Rabolt JF. Controlling Surface Morphology of Electrospun Polystyrene Fibers: Effect of Humidity and Molecular Weight in the Electrospinning Process. Macromolecules. 2004;37(2):573-8.

52. Mit-uppatham C, Nithitanakul M, Supaphol P. Ultrafine Electrospun Polyamide-6 Fibers: Effect of Solution Conditions on Morphology and Average Fiber Diameter. Macromolecular Chemistry and Physics. 2004;205(17):2327-38.

53. Collins AJ, Foley RN, Chavers B, Gilbertson D, Herzog C, Johansen K, et al. 'United States Renal Data System 2011 Annual Data Report: Atlas of chronic kidney disease & end-stage renal disease in the United States. Am J Kidney Dis. 2012;59(1 Suppl 1):A7, e1-420.

54. Ravani P, Spergel LM, Asif A, Roy-Chaudhury P, Besarab A. Clinical epidemiology of arteriovenous fistula in 2007. J Nephrol. 2007;20(2):141-9.

55. Sugimoto T, Yoshino M, Nagao M, Ishii S, Yabu H. Voltage-gated ionic channels in cultured rabbit articular chondrocytes. Comp Biochem Physiol C Pharmacol Toxicol Endocrinol. 1996;115(3):223-32.

56. Olsen JV, Ong SE, Mann M. Trypsin cleaves exclusively C-terminal to arginine and lysine residues. Mol Cell Proteomics. 2004;3(6):608-14.

57. Lee SJ, Liu J, Oh SH, Soker S, Atala A, Yoo JJ. Development of a composite vascular scaffolding system that withstands physiological vascular conditions. Biomaterials. 2008;29(19):2891-8.

58. McClure MJ, Sell SA, Simpson DG, Walpoth BH, Bowlin GL. A three-layered electrospun matrix to mimic native arterial architecture using polycaprolactone, elastin, and collagen: a preliminary study. Acta biomaterialia. 2010;6(7):2422-33.

59. Voyta JC, Via DP, Butterfield CE, Zetter BR. Identification and isolation of endothelial cells based on their increased uptake of acetylated-low density lipoprotein. J Cell Biol. 1984;99(6):2034-40.

60. Feldman HI, Kobrin S, Wasserstein A. Hemodialysis vascular access morbidity. J Am Soc Nephrol. 1996;7(4):523-35.

61. Allon M. Current management of vascular access. Clin J Am Soc Nephrol. 2007;2(4):786-800.

62. Klinkert P, Post PN, Breslau PJ, van Bockel JH. Saphenous vein versus PTFE for above-knee femoropopliteal bypass. A review of the literature. Eur J Vasc Endovasc Surg. 2004;27(4):357-62.

63. Kannan RY, Salacinski HJ, Butler PE, Hamilton G, Seifalian AM. Current status of prosthetic bypass grafts: a review. J Biomed Mater Res B Appl Biomater. 2005;74(1):570-81.

64. Rocco KA, Maxfield MW, Best CA, Dean EW, Breuer CK. In vivo applications of electrospun tissue-engineered vascular grafts: a review. Tissue engineering Part B, Reviews. 2014;20(6):628-40.

65. Huang L, Nagapudi K, Apkarian RP, Chaikof EL. Engineered collagen-PEO nanofibers and fabrics. J Biomater Sci Polym Ed. 2001;12(9):979-93.

66. L'Heureux N, Paquet S, Labbe R, Germain L, Auger FA. A completely biological tissue-engineered human blood vessel. FASEB J. 1998;12(1):47-56.

67. Girton TS, Oegema TR, Grassl ED, Isenberg BC, Tranquillo RT. Mechanisms of stiffening and strengthening in media-equivalents fabricated using glycation. J Biomech Eng. 2000;122(3):216-23.

68. Buttafoco L, Kolkman NG, Engbers-Buijtenhuijs P, Poot AA, Dijkstra PJ, Vermes I, et al. Electrospinning of collagen and elastin for tissue engineering applications. Biomaterials. 2006;27(5):724-34.

69. Wu T, Huang C, Li D, Yin A, Liu W, Wang J, et al. A multi-layered vascular scaffold with symmetrical structure by bi-directional gradient electrospinning. Colloids and surfaces B, Biointerfaces. 2015;133:179-88.

70. Nezarati RM, Eifert MB, Cosgriff-Hernandez E. Effects of humidity and solution viscosity on electrospun fiber morphology. Tissue Eng Part C Methods. 2013;19(10):810-9.

71. Croisier F, Duwez AS, Jerome C, Leonard AF, van der Werf KO, Dijkstra PJ, et al. Mechanical testing of electrospun PCL fibers. Acta biomaterialia. 2012;8(1):218-24.

72. Yin A, Zhang K, McClure MJ, Huang C, Wu J, Fang J, et al. Electrospinning collagen/chitosan/poly(L-lactic acid-co-epsilon-caprolactone) to form a vascular graft: mechanical and biological characterization. Journal of biomedical materials research Part A. 2013;101(5):1292-301.

73. Ku DN, Giddens DP, Phillips DJ, Strandness DE, Jr. Hemodynamics of the normal human carotid bifurcation: in vitro and in vivo studies. Ultrasound in medicine & biology. 1985;11(1):13-26.

74. Mrowczynski W, Mugnai D, de Valence S, Tille JC, Khabiri E, Cikirikcioglu M, et al. Porcine carotid artery replacement with biodegradable electrospun poly-e-caprolactone vascular prosthesis. Journal of vascular surgery. 2014;59(1):210-9.

75. Solan A, Dahl SL, Niklason LE. Effects of mechanical stretch on collagen and cross-linking in engineered blood vessels. Cell transplantation. 2009;18(8):915-21.

76. Kumar VA, Brewster LP, Caves JM, Chaikof EL. Tissue Engineering of Blood Vessels: Functional Requirements, Progress, and Future Challenges. Cardiovascular engineering and technology. 2011;2(3):137-48.

77. Bordenave L, Remy-Zolghadri M, Fernandez P, Bareille R, Midy D. Clinical performance of vascular grafts lined with endothelial cells. Endothelium. 1999;6(4):267-75.

78. Moll C, Reboredo J, Schwarz T, Appelt A, Schurlein S, Walles H, et al. Tissue engineering of a human 3D in vitro tumor test system. Journal of visualized experiments : JoVE. 2013(78).

79. Egger D, Spitz S, Fischer M, Handschuh S, Glosmann M, Friemert B, et al. Application of a Parallelizable Perfusion Bioreactor for Physiologic 3D Cell Culture. Cells, tissues, organs. 2017;203(5):316-26.

80. Goldstein JL, Brown MS. Atherosclerosis: the low-density lipoprotein receptor hypothesis. Metabolism. 1977;26(11):1257-75.

81. Davies PF. Hemodynamic shear stress and the endothelium in cardiovascular pathophysiology. Nat Clin Pract Cardiovasc Med. 2009;6(1):16-26.

82. Wilson SE. New alternatives in management of the infected vascular prosthesis. Surg Infect (Larchmt). 2001;2(2):171-5; discussion 5-7.

83. DeRose G, Provan JL. Infected arterial grafts: clinical manifestations and surgical management. J Cardiovasc Surg (Torino). 1984;25(1):51-7.

84. Mailloux LU, Bellucci AG, Wilkes BM, Napolitano B, Mossey RT, Lesser M, et al. Mortality in dialysis patients: analysis of the causes of death. Am J Kidney Dis. 1991;18(3):326-35.

85. Yeager RA, Porter JM. Arterial and prosthetic graft infection. Ann Vasc Surg. 1992;6(5):485-91.

86. Chudobova D, Nejdl L, Gumulec J, Krystofova O, Rodrigo MA, Kynicky J, et al. Complexes of silver(I) ions and silver phosphate nanoparticles with hyaluronic acid and/or chitosan as promising antimicrobial agents for vascular grafts. Int J Mol Sci. 2013;14(7):13592-614.

87. Siedenbiedel F, Tiller JC. Antimicrobial Polymers in Solution and on Surfaces: Overview and Functional Principles. Polymers. 2012;4(1):46.

88. Hammond PT. Engineering materials layer-by-layer: Challenges and opportunities in multilayer assembly. AIChE Journal. 2011;57(11):2928-40.

89. Friedrich J. Mechanisms of plasma polymerization–reviewed from a chemical point of view. Plasma Processes and Polymers. 2011;8(9):783-802.

90. Advincula R. Polymer brushes by anionic and cationic surface-initiated polymerization (SIP). Surface-initiated polymerization I: Springer; 2006. p. 107-36.

91. LaPlante KL, Woodmansee S. Activities of daptomycin and vancomycin alone and in combination with rifampin and gentamicin against biofilm-forming methicillin-resistant Staphylococcus aureus isolates in an experimental model of endocarditis. Antimicrob Agents Chemother. 2009;53(9):3880-6.

92. Ueng SW, Lin SS, Wang IC, Yang CY, Cheng RC, Liu SJ, et al. Efficacy of vancomycin-releasing biodegradable poly(lactide-co-glycolide) antibiotics beads for treatment of experimental bone infection due to Staphylococcus aureus. J Orthop Surg Res. 2016;11(1):52.

93. Birgand G, Radu C, Alkhoder S, Al Attar N, Raffoul R, Dilly MP, et al. Does a gentamicin-impregnated collagen sponge reduce sternal wound infections in high-risk cardiac surgery patients? Interact Cardiovasc Thorac Surg. 2013;16(2):134-41.

94. Harris LG, Richards RG. Staphylococci and implant surfaces: a review. Injury. 2006;37 Suppl 2:S3-14.

95. Kalicke T, Schierholz J, Schlegel U, Frangen TM, Koller M, Printzen G, et al. Effect on infection resistance of a local antiseptic and antibiotic coating on osteosynthesis implants: an in vitro and in vivo study. J Orthop Res. 2006;24(8):1622-40.

96. Mombelli A, Decaillet F. The characteristics of biofilms in peri-implant disease. J Clin Periodontol. 2011;38 Suppl 11:203-13.

97. Schmidmaier G, Lucke M, Wildemann B, Haas NP, Raschke M. Prophylaxis and treatment of implant-related infections by antibiotic-coated implants: a review. Injury. 2006;37 Suppl 2:S105-12.

List of figures and tables

List of figures

List of tables

Acknowledgement

This work was performed at the Chair for Tissue Engineering & Regenerative Medicine of the University of Würzburg and funded by the Interdisciplinary Centre for Clinical Research (IZKF) of the University of Würzburg. I thank all colleagues of the Research Center, as well as all people of the clinic staff, who contributed somehow to this work.

My very special gratitude goes to Prof. Dr. Heike Walles for giving me the opportunity to accomplish this work at her chair.

I want to express my gratitude to Dr.-Ing. Jan Hansmann for providing the great project and for taking the time to discuss the progress of my work. If there was any help needed, he supported me with his suggestions and content valuable discussions. I was able to learn a lot of new things under his supervision. It was a pleasure for me to work with him and his team.

I am very grateful to Prof. Dr. Rainer G. Leyh, the head of Department for Thoracic and Cardiovascular surgery, who appreciates and supports basic research at his clinic and together with Prof. Dr. Heike Walles enabled the funding of my scientific rotation.

Tobias Weigel did an incredible job explaining the electrospinning setup to me. His help with SEM imaging and guiding in mechanical tests was most valuable. Many thanks therefore.

Tobias and Sebastian Schürlein also had enough time for any discussions about the topic and they always shared their experience with me. Many thanks to Thomas Schwarz for CAD designs.

I would also like to thank all other members of the AG Hansmann and the members of the bioreactors meeting for many constructive discussions and a lot of helpful suggestions. Thank you all for welcoming me so nicely and providing such a great atmosphere, and for great chats, distractions and a lot of fun in the lab.

Further thanks to my parents, my late father who keeps inspiring me and mom for being proud of me and supporting me as much as she can. Thank to my brother for his advices. And I want to thank my Ana from bottom of my heart for her love, great support and so many things that we manage together.